



Analysis of radiation emission from MYRRHA spent fuel and implications for non-destructive safeguards verification



M. Preston^{a,*}, A. Borella^b, E. Branger^a, S. Grape^a, R. Rossa^b

^a Division of Applied Nuclear Physics, Department of Physics and Astronomy, Uppsala University, Uppsala, Sweden

^b Environment, Health and Safety Institute, SCK CEN Belgian Nuclear Research Centre, Mol, Belgium

ARTICLE INFO

Article history:

Received 12 March 2021

Received in revised form 15 June 2021

Accepted 27 June 2021

Available online 14 July 2021

Keywords:

MYRRHA

Fuel depletion

Simulation

Nuclear safeguards

Fast reactor

Non-destructive assay (NDA)

ABSTRACT

The radionuclide composition of, and emitted radiation in, spent nuclear fuel from the future MYRRHA facility have been studied using depletion simulations to understand potential consequences for safeguards verification using non-destructive assay. The simulations show that both the gamma-ray and neutron emission rates in spent MYRRHA assemblies are lower than in spent PWR UO₂ and MOX assemblies. In addition, gamma-ray emission rates from ¹³⁴Cs and ¹⁵⁴Eu are considerably lower, and the total neutron emission rate in MYRRHA fuel is much less sensitive to fuel burnup and cooling time. The main reason is that the fast neutron spectrum in MYRRHA affects the radionuclide production in the fuel. One result is that ²⁴⁴Cm, the main contributor to the neutron emission in spent light water reactor fuel, has a limited production in MYRRHA. Consequently, neutron-detection techniques could be used to more directly assay the plutonium content of spent MYRRHA fuel.

© 2021 The Author(s). Published by Elsevier Ltd. This is an open access article under the CC BY license (<http://creativecommons.org/licenses/by/4.0/>).

1. Introduction

Non-destructive assay (NDA) techniques based on gamma-ray and neutron detection are important in safeguards verification of spent nuclear fuel (SNF) (Phillips, 1991; International Atomic Energy Agency, 2011). NDA measurements are used in the verification of the completeness and correctness of operator declarations, and determination of fuel parameters such as initial enrichment (IE), burnup (BU) and cooling time (CT) can be of interest (Tobin et al., 2012). With different types of Generation IV nuclear energy systems on the horizon (Locatelli et al., 2013), appropriate safeguards techniques must be identified and developed (Durst et al., 2007; Grape et al., 2014). In this paper we present a step in this direction, focussing on SNF from the upcoming MYRRHA (Multi-purpose hYbrid Research Reactor for High-tech Applications) facility at SCK CEN in Mol, Belgium (Ait Abderrahim et al., 2012), expected to be fully operational by 2036. MYRRHA will be an accelerator-driven system, with a 600-MeV proton linear accelerator coupled to a sub-critical reactor core and a spallation target in the reactor core. It can be operated in critical or sub-critical mode, with only the latter requiring spallation neutrons to sustain the neutron chain reaction. Here, we consider only SNF assemblies from the critical mode of MYRRHA.

The properties of MYRRHA and its fuel present several differences compared to typical light water reactor (LWR) fuel often verified in safeguards: MYRRHA will contain mixed-oxide (MOX) fuel with an initial plutonium content of 30%, cooled by lead–bismuth eutectic (LBE) (Van den Eynde et al., 2015). The initial fuel composition and fast neutron energy spectrum in MYRRHA will affect the SNF radionuclide inventory, and could have implications for selecting appropriate NDA techniques. To study the potential for verification of MYRRHA fuel using gamma rays and neutrons, this paper presents results from depletion simulations of the MYRRHA fuel, performed using the Monte Carlo neutronics Serpent2 code (Leppänen et al., 2013). The results include the expected gamma-ray and neutron emissions in an SNF assembly and the build-up of radionuclides in the fuel. Throughout the paper, the results are compared with recent depletion simulations of uranium oxide (UO₂) and MOX fuel in a representative pressurised water reactor (PWR) (Elter et al., 2020). This comparison allows analysing differences between both fuel type and reactor type, particularly highlighting the safeguards implications for verification of MYRRHA fuel.

In Table 1, some key parameters of the MYRRHA fuel are summarised and compared to UO₂ and MOX fuel of a PWR. These parameters include properties of interest for safeguards, such as the amount of low enriched uranium (LEU) and plutonium in the fresh and spent fuel. Some key differences between fuel in MYRRHA and fuel in commercial PWRs are clear: the MYRRHA fuel

* Corresponding author.

E-mail address: markus.preston@physics.uu.se (M. Preston).

Table 1

Some key properties of MYRRHA and light-water reactor fuel relevant for safeguards. The PWR fuel dimensions are representative values for Westinghouse 17×17 FAs, taken from (Baron et al., 2020), whereas the MYRRHA fuel dimensions were taken from Van den Eynde et al. (2015) and Van Tichelen et al. (2020). The average PWR discharge burnups were obtained from U.S. Energy Information Administration (2021) and the MYRRHA discharge burnup from Van den Eynde et al. (2015). The plutonium and ^{235}U content before and after irradiation were determined from the depletion simulations detailed later in this paper and are given both in terms of absolute mass and significant quantities (1 SQ = 8 kg plutonium or 75 kg LEU (International Atomic Energy Agency, 2001)).

Property	Fuel type		
	PWR-UO ₂	PWR-MOX	MYRRHA
Initial enrichment/ Initial Pu content [wt.%]	4	9	30
Core power	1,300 MW _e	1,300 MW _e	96 MW _{th} ¹
Coolant	Water	Water	Liquid Pb-Bi eutectic (LBE)
Number of assemblies in core	193	193	108 ¹
Active fuel length [cm]	427	427	65
Number of fuel rods per assembly	264	264	127
Average discharge burnup [MWd/kgHM]	40	40	60
LEU ($^{235}\text{U} + ^{238}\text{U}$) content in fresh fuel			
Per assembly [kg]	550	500	12
Per assembly [SQ]	7.3	6.7	0.16
Per core [SQ]	1400	1300	17
LEU ($^{235}\text{U} + ^{238}\text{U}$) content at discharge			
Per assembly [kg]	520	490	11
Per assembly [SQ]	6.9	6.5	0.15
Per core [SQ]	1300	1200	16
Plutonium content in fresh fuel			
Per assembly [kg]	0	50	5.1
Per assembly [SQ]	0	6.2	0.64
Per core [SQ]	0	1200	69
Plutonium content at discharge			
Per assembly [kg]	6.7	40	4.5
Per assembly [SQ]	0.84	5.0	0.57
Per core [SQ]	160	970	61

¹ In the critical configuration. For the sub-critical configuration, the core will contain 72 assemblies and have a power of 70 MW_{th} (Van den Eynde et al., 2015).

assemblies (FAs) will be considerably shorter and contain fewer fuel rods. As a result, the amount of plutonium per assembly is in any case smaller for MYRRHA than for a PWR MOX FA used in a typical commercial reactor. The listed IE and initial plutonium contents (IPCs) are the values assumed throughout this work.

Different NDA techniques for radiation measurements of fast-reactor SNF have been investigated in the past. These include gamma-ray scanning (Barnes et al., 1979; Phillips et al., 1979) or neutron-coincidence counting (Persiani and Gundy, 1982) for BU determination, active neutron counting for fissile-mass determination (Persiani and Gundy, 1982), and neutron-coincidence counting (Lestone et al., 2002) or neutron resonance densitometry (Neutron Self-Indication Assay of SEFOR Fuel Rods, 1969; Neutron Self-Indication Assay of SEFOR Fuel Rods, 1969) for plutonium-mass determination. Although there are several differences between the reactors in these studies and MYRRHA (e. g. core power, core size, fuel composition), these studies show some important differences between the radiation signatures from fast-reactor and thermal-reactor SNF. These include a more important direct contribution from the plutonium isotopes to the total neutron emission in fast-reactor SNF (Persiani and Gundy, 1982; Lestone et al., 2002). In addition, differences between the gamma signatures from fast-reactor and thermal-reactor SNF have been highlighted in the field of nuclear forensics (Osborn, 2018; Chirayath et al., 2018), although these studies only considered very low BU values. In this paper, we study the differences in radiation emissions and

radionuclide inventory with respect to LWR SNF in a more systematic way in the context of safeguards.

Due to the ongoing interest in developing Generation IV nuclear energy systems, there is a need to assess the performance of several types of NDA instrumentation and analysis methodologies to these case studies. Because today's NDA instrumentation is mainly developed for LWR safeguards verification, it is reasonable to make a systematic comparison between the gamma-ray and neutron emissions and radionuclide inventories in SNF from different reactor types. Several libraries containing results from LWR depletion simulations have been developed to facilitate modelling of next-generation NDA instruments (see for example Elter et al., 2020; Rossa and Borella, 2020; Galloway et al., 2012; Henzl, 2014), and this paper presents the first step towards such a library also for MYRRHA SNF.

2. Simulation framework

Depletion simulations have been performed using Serpent2 (Leppänen et al., 2013), which is a Monte-Carlo-based code for modelling of nuclear reactors and radiation transport. Serpent2 includes extensive depletion-simulation capabilities, where the evolution of the radionuclide composition of fuel is determined by combining Monte Carlo determinations of the reactor core neutron fluence rate with the deterministic Bateman equations. After discharge from the core, a neutron fluence rate of zero is assumed so that the Bateman equations only depend on radioactive decay. Using this methodology, the radionuclide composition of the fuel can be estimated at different BUs and at different CTs after discharge from the core.

In the present work, Serpent2.1.31 has been used to simulate fuel depletion in the critical MYRRHA core¹. In these simulations, a radially and axially infinite lattice has been assumed, meaning that the radial dimensions of a single fuel-pin cell (i. e. the fuel, the cladding and the coolant) were defined and replicated using reflective boundary conditions. The neutron-transport simulations were performed using the *k*-eigenvalue criticality source method, where the number of initial source neutrons per cycle as well as the number of inactive and active cycles have to be specified. By studying the dependence of the modelled infinite multiplication factor k_{∞} on these three parameters, it was found that using 10 inactive and 100 active cycles consisting of 5000 initial neutrons per cycle resulted in a solution with good precision and accuracy. The uncertainty on k_{∞} ranged between 71 and 85 pcm for the simulated irradiation histories. This configuration was also used in the recent development of a LWR SNF library (Elter et al., 2020). The neutron cross-section data, the fission-product yields and the radioactive-decay data used in the simulations were obtained from the JEFF-3.3 library (Plompen et al., 2020).

2.1. Fuel pin geometry and initial composition

Because existing safeguards instrumentation has been developed and designed mainly for LWR fuel, it is relevant to compare results on MYRRHA fuel properties (radiation emission and radionuclide composition) with those of LWR fuel. Recent results from depletion simulations of PWR UO₂ (initial enrichment 4%) and MOX (initial plutonium content 9%) fuel (Elter et al., 2020) are used here for this comparison. This allows analysing how different fuel compositions (in particular the plutonium content) and different neutron energy spectra affect fuel depletion and what

¹ When fully operational, the MYRRHA facility can also be operated in sub-critical mode, where a proton accelerator is used to sustain the neutron chain reaction in the core.

potential implications this has for safeguards verification of MYRRHA SNF. Fig. 1 shows the neutron energy spectra in the three types of fuel at the beginning of irradiation. Note that in addition to the LWR data in Elter et al. (2020), the associated Serpent2 input files were made available to us so that additional parameters of the LWR simulation could be determined when necessary. The simulations of the PWR fuel were also performed using Serpent2 assuming a radially and axially infinite lattice. The PWR models did not include soluble boron in the moderator, burnable poison rods or control rods, which could affect the neutron energy spectrum and therefore the radionuclide composition of the spent fuel. The impact of these and other parameters has been investigated previously (Rossa et al., 2013; Hu et al., 2014). In Rossa et al. (2013), it was found that adding soluble boron to the moderator in an infinite-lattice model increased the production of actinides in PWR UO₂ fuel by up to 20% relative to the case with no boron at BU up to 40 MWd/kgHM. In Hu et al. (2014), the presence of burnable poison rods were found to decrease the production of several radionuclides of interest for the present work by up to 8%. It is clear that parameters such as these will have some impact on both the radionuclide composition and the radiation emission. As described in Henzl (2014), including these and other effects in a library of modelled spent fuel assemblies can be important when performing detailed studies of the response of a realistic NDA system to a particular fuel assembly. For this work, however, the objective is rather to highlight key differences between different fuel types for different BUs and CTs. With this objective in mind, the infinite-lattice model was determined to be sufficient.

The geometries of the fuel-pin cells in the MYRRHA and PWR simulations, as well as the properties of the respective cladding and coolant materials, are shown in Table 2. The assumed cladding, coolant and fuel temperatures in the MYRRHA case were taken from Jaluvka (2015). The material temperatures affect the cross sections due to broadening of resonance peaks in neutron interaction cross sections. In the MYRRHA depletion simulations, the “Doppler preprocessor” functionality of Serpent2 was used to incorporate these effects into the cross-section data.

In this work, an IPC of 30 wt.% (relative to all heavy metal in the fresh fuel) was assumed for the MYRRHA fuel. This is the expected IPC when using MOX fuel in MYRRHA (Van den Eynde et al., 2015). This is however not the only type of fuel that could be used in MYRRHA – highly enriched uranium (HEU) oxide fuel or various uranium and plutonium metal fuels have also been considered (Ait Abderrahim et al., 2005). In addition, fuel containing minor actinides could be used for transmutation of radioactive waste (Mueller, 2013). Nonetheless, the 30% MOX fuel assumed in this work does in itself present a larger challenge to safeguards than HEU fuel, due to the smaller mass of one SQ of plutonium and the more complex composition of MOX fuel. Because methods for safeguarding all types of SNF at MYRRHA will eventually be required, it is relevant to initially consider a more challenging scenario as a baseline for MYRRHA safeguards. The assumed initial fuel composition in this work is shown in Table 3 together with the compositions of the reference PWR fuels used in the comparison. Note that the assumed MYRRHA fuel composition includes natural (not depleted) uranium. The density of the fuel oxide was assumed to be 10.16 g/cm³, calculated from Stankus et al. (2008) assuming a density 95% of the theoretical oxide density.

In this work, we focus on the scenario where a SNF assembly is to be verified after discharge from the MYRRHA core. The percentage of total fissile material as well as plutonium in MYRRHA fuel will be high compared to typical LWR fuel, and stresses the need for efficient and accurate safeguards measures. While the composition of the plutonium in the fuel affects the attractiveness for proliferation (Bathke et al., 2011), all plutonium isotopes are treated the same by the International Atomic Energy Agency

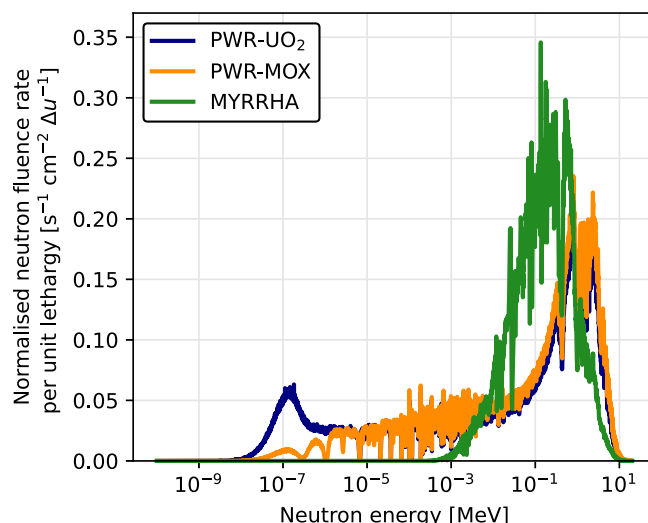


Fig. 1. The neutron energy spectra in the modelled PWR and MYRRHA fuels at the beginning of irradiation. The integral of each spectrum has been normalised to one.

Table 2

Geometry of the simulated MYRRHA fuel cell, compared to the reference PWR fuels from Elter et al. (2020). The MYRRHA fuel geometry was obtained from Kennedy et al. (2020) and the cladding, coolant and fuel temperatures from Jaluvka (2015).

Parameter	MYRRHA fuel (this work)	PWR fuels ¹
Pin radius [cm] ²	0.33	0.48
Cell geometry	Hexagonal	Square
Pin pitch [cm]	0.84	1.26
Cladding material	DIN1.4970 steel	Natural Zr
Cladding density [g/cm ³]	7.95	6.52
Cladding temperature	633.15	900
Coolant material	Lead–bismuth eutectic (LBE)	Water (H ₂ O)
Coolant density [g/cm ³]	10.3	0.75
Coolant temperature [K]	633.15	600
Fuel temperature [K]	1473.15	1500

¹ The geometry parameters were identical for the UO₂ and MOX fuels.

² The pin radius including the cladding.

Table 3

Assumed composition (in weight percentage) of fresh fuel in the MYRRHA depletion simulation and in the reference PWR cases. The PWR fuel compositions were obtained from Elter et al. (2020).

Isotope	MYRRHA	PWR-UO ₂	PWR-MOX
²³⁴ U [wt.%]	0	0	0.00096
²³⁵ U [wt.%]	0.44	3.53	0.20
²³⁸ U [wt.%]	61.39	84.62	80.02
²³⁸ Pu [wt.%]	0.061	0	0.20
²³⁹ Pu [wt.%]	17.98	0	4.34
²⁴⁰ Pu [wt.%]	6.91	0	2.07
²⁴¹ Pu [wt.%]	1.22	0	0.75
²⁴² Pu [wt.%]	0.32	0	0.57
¹⁶ O [wt.%]	11.67	11.85	11.84
Oxide density [g/cm ³]	10.16	10.5	10.5

(International Atomic Energy Agency, 2001). In this work, we therefore consider both the total amount of plutonium in the fuel and the radiation emitted from the individual plutonium isotopes.

2.2. Irradiation conditions

During equilibrium conditions, the critical configuration of the MYRRHA core consists of 108 FAs, each containing 127 fuel rods (Van Tichelen et al., 2020). The operating schedule in MYRRHA is foreseen to consist of 90-day irradiation cycles followed by down-

times to allow maintenance and re-shuffling of the FAs (Gelineau and Gavrilov, 2012). As shown in Fig. 2, the duration of the downtimes will alternate between 30 and 90 days.

The 108 assemblies of the critical configuration are divided into 18 batches of six, which are re-shuffled at the end of each operating cycle. At its end of life, a single FA will have gone through 18 90-day cycles, reaching a discharge BU of approximately 60 MWd/kgHM (Van den Eynde et al., 2015). In the depletion simulations, these were the assumed irradiation conditions. A constant power of 76.7 W/cm in the fuel was assumed throughout all cycles. The simulation was performed in time steps of 15 days, corresponding to BU steps of 0.56 MWd/kgHM. The cooling of the fuel after discharge was simulated in time steps of 90 days up to 10 years, then in steps of 180 days up to 40 years.

In MYRRHA, both fresh and spent fuel will be stored in the in-vessel fuel storage (IVFS) to minimise delays between operation cycles (Di Maria et al., 2012). Re-shuffling of fuel, and insertion of fresh fuel, will be done using two in-vessel fuel handling machines so that the vessel will not have to be opened. However, when all fresh fuel in the IVFS has been replaced by spent fuel, the vessel will be opened so that SNF can be removed from the IVFS and replaced by fresh fuel for subsequent cycles. It is at this point that one may foresee the first direct access to SNF from MYRRHA, and that this is where fuel verification could be performed. We assume that under normal operating conditions, the fuel that is to be verified will have been fully burned through 18 cycles to reach 60 MWd/kgHM. These assemblies will have a range of CTs, but here we assume that all have been in the IVFS for at least some time so that the minimum CT before an NDA measurement is possible is approximately three months². For this reason, radionuclides with half lives shorter than one month were not considered in this publication, but may be included in future work.

3. Results

To understand how to verify SNF from MYRRHA using NDA techniques, the characteristics of the emitted radiation to be detected by safeguards instruments must first be understood. In this work we focus on the passive emission of gamma rays and neutrons in the SNF and its dependence on the radionuclide inventory, and analyse how and to what extent it differs from LWR fuel currently under safeguards. For the radiation emission, we only consider the radioactive decay within the SNF rods – the transport of the emitted radiation within the FA or to a potential detector is not included since designs and positioning of future detector stations have not yet been looked into. In a realistic scenario, effects such as scattering and attenuation will affect the detectable radiation signatures, but the more fundamental properties of the emitted radiation nonetheless provide valuable input to such analyses and assessments. In most cases, the results are shown for several values of BU and CT, but when specific discharge BUs are assumed a value of 60 MWd/kgHM is used for MYRRHA and 40 MWd/kgHM for the PWR fuels. A discharge BU of 40 MWd/kgHM is representative for PWR fuels verified in safeguards today (U.S. Energy Information Administration, 2021). It is however important to note that the discharge burnup may vary along the axial length of the fuel assembly, locally reaching values considerably higher than the average.

The amount of fuel material in the assembly was taken into account by scaling the gamma-ray and neutron emission rate by the number of rods per assembly. The resulting emission rates

per assembly axial length may be compared with the PWR results where both the fuel-rod diameter and the assembly size are larger (see Tables 1 and 2). It is worth emphasising that because the rates were determined per axial length, any difference between the determined emissions in MYRRHA and the PWR fuels will partly be due to the fact that there is less heavy metal per assembly axial length in the MYRRHA fuel.

3.1. Gamma-ray emission

3.1.1. Total gamma-ray emission

The total gamma-ray emission rate in a single FA was determined using the radioactive-decay source mode of Serpent, where the energies and intensities of the emissions from all radionuclides in the SNF were determined. In previous spectroscopic measurements on LWR SNF at the Swedish interim storage for SNF, Clab, only peaks above approximately 500 keV in the gamma-ray energy spectrum were analysed (Vaccaro et al., 2016) because gamma-ray scattering and attenuation between the SNF and detector resulted in a significant low-energy background. Although the measurement conditions during verification of MYRRHA fuel are not defined yet, and may come to differ from those during LWR fuel verification, we here consider gamma rays with an energy above 500 keV. Fig. 3 shows the total gamma-ray emission rate above 500 keV as a function of the CT after discharge, for three different BUs: 20, 40 and 60 MWd/kgHM. These values were chosen to represent low, medium and full BU in the PWR and MYRRHA cases.

From Fig. 3, it can be seen that the total gamma-ray emission rate in a MYRRHA SNF assembly is approximately ten times lower than in a PWR SNF assembly. This is partly due to the thicker fuel rods and larger assemblies in the PWR cases, i. e. that the amount of fuel material per assembly axial length is considerably lower in the MYRRHA fuel than in the PWR fuels (as discussed above). Another reason for the differences in the emission rate could be due to differences in the radionuclide composition of the SNF, as discussed below. The lower total gamma-ray emission rate per axial length in the MYRRHA fuel either means that longer measurement times will be required to reach the same statistical accuracy as in NDA of PWR fuel, or that the count rate should be increased by decreasing the fuel-detector distance or thickness of attenuating material.

3.1.2. Potential for detecting gamma rays below 500 keV

Although only gamma-ray emissions above 500 keV have been considered in this paper, it is worth pointing out that also photons with lower energies (including x-rays) may be of interest in NDA measurements. Of special interest are gamma rays emitted after α decays of uranium and plutonium isotopes, which would allow directly assaying the uranium and plutonium content of the fuel (Sampson, 1991). Typically, the very high photon background caused by decaying fission products completely obscures these gamma rays in a spectroscopic measurement on SNF (Phillips, 1991). However, the higher plutonium content in MYRRHA fuel compared to PWR fuel as well as the thinner fuel rods in the MYRRHA case (resulting in a lower self-absorption of gamma rays) suggest that detecting photons from plutonium decays could be more feasible in the case of MYRRHA fuel. As an example we consider the ^{239}Pu 375-keV gamma-ray emission, which is one of the more intense emissions from that isotope. Because the major contributor to the background when attempting to measure low-energy photons from SNF is the 662-keV line from ^{137}Cs (and its associated Compton continuum), it is relevant to compare the intensities of these two emissions. Fig. 4 shows the ratio between these two emission rates in PWR and MYRRHA fuel as a function of the CT after discharge, for three different BUs (to highlight the BU- and CT-dependence of the gamma-ray emission rate). It is clear that

² Since the vessel can be opened during the 90-day downtimes, it is in principle possible that shorter-cooled fuel can be discharged as well, although we do not investigate those cases in this work.

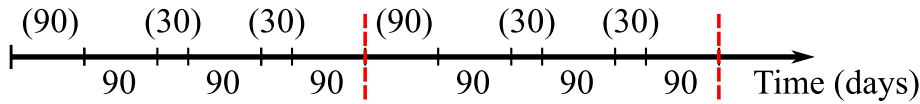


Fig. 2. MYRRHA operating schedule assumed in this work. Each irradiation cycle is 90 days long, followed by downtimes of 30 or 90 days (in parentheses). Each FA in the core will be irradiated for 18 active cycles, resulting in a total irradiation time of 1620 days per assembly. The region between the two red dashed lines indicate the part of the schedule that is repeated throughout operations.

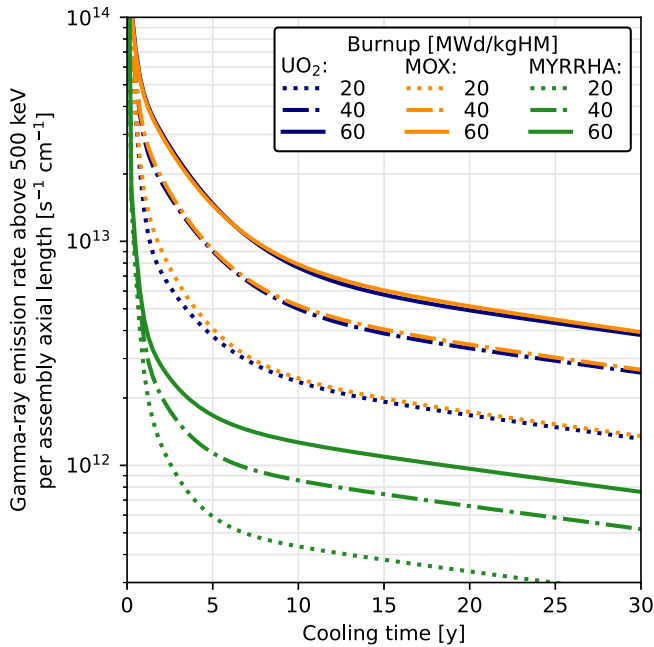


Fig. 3. The total gamma-ray emission rates above 500 keV per assembly axial length of MYRRHA and PWR fuel, as functions of the cooling time after discharge for three different burnups: 20, 40 and 60 MWd/kgHM.

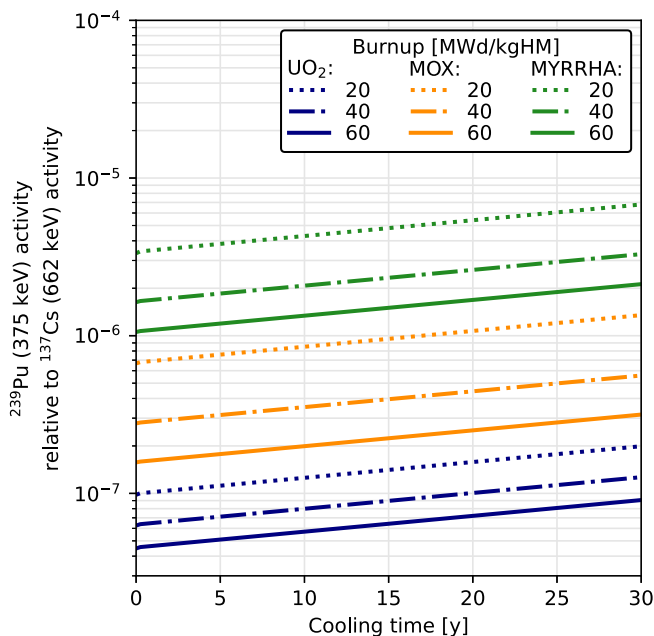


Fig. 4. The intensity of the 375-keV emission from ^{239}Pu relative to the intensity of the 662-keV emission from ^{137}Cs for MYRRHA and PWR fuel, as functions of the cooling time after discharge for three different burnups. The relative strength of the 375-keV emission in MYRRHA fuel is approximately 50 times that in UO_2 fuel.

the relative intensity of the plutonium emission is approximately 50 times larger in the MYRRHA case than in the UO_2 case, but still very much weaker (by a factor of up to 10^6) than the 662-keV emission from ^{137}Cs . Further work is needed to evaluate the effects of the measurement conditions and chosen NDA instrumentation on the possibilities to detect such low-energy gamma rays. Therefore, we now turn our focus back to the gamma-ray emissions above 500 keV.

3.1.3. Fission-product contributions to the gamma-ray emission above 500 keV

The majority of the gamma-rays emitted from SNF are due to decaying fission products, which may be used as indicators of fuel parameters such as IE, BU and CT. The energy threshold of 500 keV was the first criterion for selecting relevant gamma-emitting radionuclides. Second, requirements based on nuclide half-life and sufficient branching ratio for gamma-ray emission can be introduced. Additionally, the mean free path of photons increases with energy, meaning that high-energy gamma rays are more likely to reach the detector and can also provide more information about the interior of the assembly (Jansson, 2002). High-energy gamma rays are therefore especially interesting for fuel-verification purposes. Instead of analysing these selection criteria separately, we study the fractional contribution of all radionuclides to the total gamma-ray emission rate above 500 keV as a function of the CT after discharge. Fig. 5 shows the relative contributions for the two PWR cases and MYRRHA, where all radionuclides that contribute with at least 1% of the total emission rate above 500 keV from MYRRHA SNF with a BU of 60 MWd/kgHM at any CT between 6 months and 30 years are shown explicitly. The absolute emission rates from these radionuclides in MYRRHA fuel, which are of interest when considering e.g. achievable count rates in an NDA measurement, are shown in Table 4.

The eight nuclides shown in Fig. 5 – ^{95}Nb , ^{95}Zr , ^{144}Ce , ^{106}Ru , ^{134}Cs , ^{125}Sb , ^{154}Eu and ^{137}Cs – have previously been suggested as indicators of BU and/or CT of SNF (Hsue et al., 1978; Phillips, 1991a; International Atomic Energy Agency, 1992). The measured intensities of ^{134}Cs , ^{154}Eu and ^{137}Cs and/or ratios between them are perhaps the most well-known BU indicators, especially for longer-cooled fuel (Phillips, 1991b). Of the gamma-ray emitters considered in this work, ^{125}Sb is possibly the one least often suggested in the context of safeguards – the reason for this could be that its fission yield is considerably smaller in uranium than in plutonium (Plompen et al., 2020) and that it is therefore not a major contributor to the gamma-ray rate from UO_2 (i.e. the majority of LWR fuel worldwide). Indeed, it is clear from Fig. 5 that the relative contribution from ^{125}Sb exceeds 1% only in the MYRRHA case. The most prominent gamma-ray emissions from the selected nuclides are listed in Table 5.

All nuclides listed in Table 5 are produced as a result of fission in the fuel, some as direct fission product and some as the result of one or more subsequent neutron captures in direct fission products. The build-up of these radionuclides during operation of MYRRHA is expected to differ from that in a LWR for four main reasons:

- The higher plutonium content in the MYRRHA fuel means that plutonium isotopes will constitute a higher fraction of the fissioning nuclei, affecting the fission yields.

- The fast neutron energy spectrum in the MYRRHA core will result in different fission-product distributions compared to a thermal LWR core.
- Neutron-capture cross sections typically decrease as the neutron energy increases, so that neutron capture is generally less probable in the MYRRHA core for a given neutron fluence rate.
- The neutron fluence rate is higher in MYRRHA than in a LWR, but this often does not compensate for the decrease in the capture cross section. This can result in a lower neutron capture rate per fission in MYRRHA fuel as compared to LWR fuel.

Based on Fig. 5, some particularly interesting differences between the contributions to gamma-ray emission in MYRRHA and PWR fuel should be noted. First, ^{137}Cs starts to dominate the emission in MYRRHA SNF at shorter CTs than in the PWR SNF. Second, the relative contributions of ^{134}Cs and ^{154}Eu are considerably reduced in the MYRRHA fuel. As mentioned above, these nuclides are well-known in passive gamma spectroscopy measurements on LWR SNF, and their reduced contribution could have consequences for MYRRHA safeguards.

3.1.4. Fission-product inventory

To explain the differences between the gamma-ray emission in MYRRHA and PWR fuel, one can study the build-up of the fission products in Table 5 during operation of the reactor core. Fig. 6a shows the fission-product number densities (the number of nuclei per cm^3) as functions of BU in MYRRHA and PWR fuel, obtained from Serpent simulations. We first consider three radionuclides with a half life of less than one year: ^{95}Nb , ^{95}Zr and ^{144}Ce . The build-up of these radionuclides is highly dependent on the irradiation scheme (because significant decays occur even during the 30-day outages between consecutive irradiation periods). Discontinuities in the build-up are therefore due to the simulated irradiation histories of the fuel. Even though the assumed irradiation history in MYRRHA is different from the one in the PWR cases, the build-up of these three radionuclides is rather similar because the fission yields are similar in UO_2 and MOX fuels, and also in a thermal and a fast neutron energy spectrum (Plompen et al., 2020).

For the radionuclides with half lives between one and five years (^{106}Ru , ^{134}Cs and ^{125}Sb), some dependency on the irradiation scheme can be seen. The build-up of ^{106}Ru in MYRRHA is rather similar to that in PWR MOX, but differs significantly from the PWR UO_2 case. This can be attributed to the fact that the cumulative fission yield for ^{106}Ru is 0.41% in thermal-neutron induced fission of ^{235}U , 4.3% in thermal-neutron induced fission of ^{239}Pu and 4.0% in fast-neutron³ induced fission of ^{239}Pu (Plompen et al., 2020). The main difference therefore lies in the fissioning nuclide, and not the neutron energy spectrum. ^{134}Cs is on the other hand produced to a much lesser extent in MYRRHA compared to both PWR cases. The reason for this is that ^{134}Cs is not primarily produced as a direct fission product, but by neutron captures by the much more common fission product ^{133}Cs (Phillips, 1991b). The cumulative fission yield for ^{133}Cs is similar for fast and thermal neutrons as well as for different fissioning nuclides, but the cross section for neutron capture by ^{133}Cs decreases rapidly with neutron energy (Plompen et al., 2020). Therefore, the neutron energy spectrum in MYRRHA is not as efficient in producing ^{134}Cs as a thermal spectrum. ^{125}Sb , on the other hand, is a direct fission product. The main reason for the difference in build-up is again the main fissioning nuclide, not the neutron energy spectrum – the cumulative fission yield of ^{125}Sb is 0.030% in thermal-neutron induced ^{235}U fission, 0.11% in thermal-neutron induced ^{239}Pu fission and 0.14% in fast-neutron induced ^{239}Pu fission.

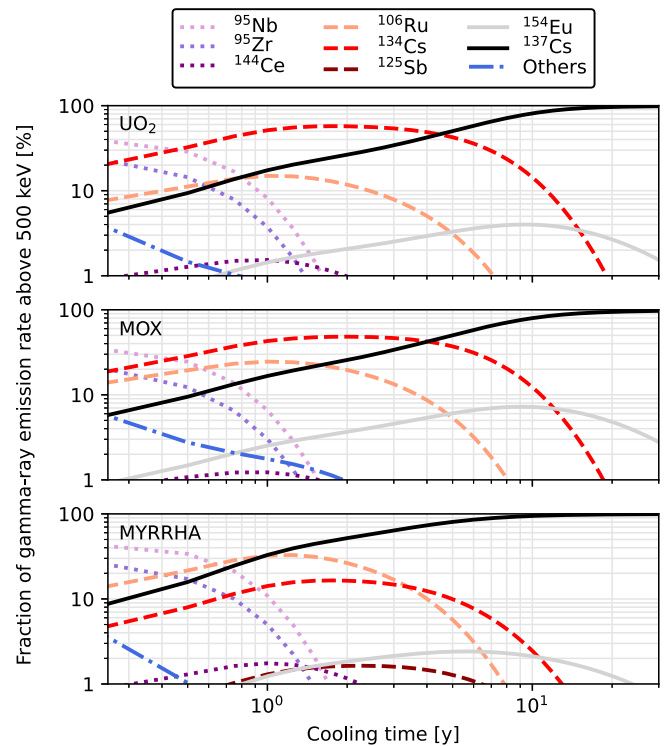


Fig. 5. The relative contributions to the gamma-ray emission rate above 500 keV from eight radionuclides in the PWR UO_2 and MOX cases (both at a discharge burnup of 40 MWd/kgHM) and MYRRHA (at a discharge burnup of 60 MWd/kgHM) as functions of the cooling time after discharge.

Finally, we consider the fission products with half lives above five years. As with ^{134}Cs , ^{154}Eu is not primarily produced as a direct fission product. Its build-up in the fuel is quite complex, as it can proceed through several different chains of neutron captures and β decays in fission products (Håkansson et al., 1995). To understand why the build-up of this nuclide in MYRRHA fuel differs from the PWR cases, the so-called depletion matrix used in the Serpent simulation was studied for the nuclides relevant for ^{154}Eu production. This matrix contains the reaction cross sections and decay parameters needed to solve the Bateman equations at each time step in the depletion simulation, and therefore describes the probabilities governing the radionuclide build-up. It was found that the probability for neutron capture in all nuclei that could contribute to ^{154}Eu production is on average ten times smaller in the MYRRHA fuel than in the UO_2 fuel – again, due to the fast neutron energy spectrum. This is also true for ^{153}Eu , the direct precursor of ^{154}Eu . Following the same argument as above, the probability for neutron capture is less likely in MYRRHA, suppressing the production of ^{154}Eu . It is also worth pointing out that ^{149}Sm , a nuclide in the ^{154}Eu production chains, is a well-known thermal-neutron absorber. The capture cross section for this nuclide is several orders of magnitude smaller at fast neutron energies (Plompen et al., 2020), which significantly reduces the impact of this reaction in MYRRHA, and potentially leads to a less complex ^{154}Eu production mechanism. ^{137}Cs is perhaps the most commonly used radionuclide in nuclear safeguards, and as shown here its production in MYRRHA is very similar to both PWR cases. This is a result of it being a direct fission product with a fission yield quite similar for thermal- and fast-neutron induced fission in ^{235}U and ^{239}Pu . The neutron-capture cross section for ^{137}Cs is similar for fast and thermal neutrons (Plompen et al., 2020), and small enough that loss of ^{137}Cs through neutron capture is negligible. Therefore, the common assumption that the ^{137}Cs build-up has a linear depen-

³ Here, “fast neutrons” refers to 400-keV neutrons.

Table 4

Radionuclide contributions to the total gamma-ray emission rate above 500 keV in a MYRRHA FA with a discharge burnup of 60 MWd/kgHM. Only rates at cooling times below 20 nuclide half lives are shown.

Cooling time [y]	Gamma-ray emission rate > 500 keV per assembly axial length [$10^{10} \text{ s}^{-1} \text{ cm}^{-1}$]								
	⁹⁵ Nb	⁹⁵ Zr	¹⁴⁴ Ce	¹⁰⁶ Ru	¹³⁴ Cs	¹²⁵ Sb	¹⁵⁴ Eu	¹³⁷ Cs	Others
1	49	22	7.8	140	64	5.8	5.5	150	1.7
5	–	–	0.22	9.5	17	2.1	4.0	130	0.16
10	–	–	$2.7 \cdot 10^{-3}$	0.32	3.1	0.61	2.7	120	0.10
20	–	–	–	$3.5 \cdot 10^{-4}$	0.11	0.049	1.2	95	0.061
30	–	–	–	–	$3.8 \cdot 10^{-3}$	$4.0 \cdot 10^{-3}$	0.54	76	0.037

Table 5

Half lives and important emissions of the gamma-emitting fission products selected for analysis in this work. Data taken from [Plompen et al. \(2020\)](#).

Isotope	Half-life	Gamma-ray energy [MeV]	Intensity [% decay ⁻¹]
⁹⁵ Nb	35 days	0.766	99.8
⁹⁵ Zr	64 days	0.724, 0.757	44.3, 54.4
¹⁴⁴ Ce ¹	285 days	0.697, 1.489, 2.186	1.41, 0.286, 0.73
¹⁰⁶ Ru ²	372 days	0.512, 0.622, 1.050, 1.128, 1.562, 1.766, 1.797, 1.988, 2.112, 2.366	20.5, 9.87, 1.49, 0.40, 0.156, 0.03, 0.0274, 0.0258, 0.0351, 0.0232
¹³⁴ Cs	2.064 y	0.563, 0.569, 0.605, 0.796, 0.802, 1.038, 1.168, 1.365	8.34, 15.37, 97.63, 85.47, 8.69, 0.99, 1.79, 3.02
¹²⁵ Sb	2.76 y	0.601, 0.607, 0.636, 0.671	17.76, 5.02, 11.32, 1.78
¹⁵⁴ Eu	8.60 y	0.592, 0.723, 0.757, 0.873, 0.996, 1.005, 1.274, 1.494, 1.596	4.95, 20.05, 4.53, 12.17, 10.5, 17.86, 34.89, 0.70, 1.78
¹³⁷ Cs ³	30.1 y	0.662	85.1

¹ Gamma rays emitted after the β^- decay of the short-lived daughter ¹⁴⁴Pr ($t_{1/2} = 17.3$ min).

² Gamma rays emitted after the β^- decay of the short-lived daughter ¹⁰⁶Rh ($t_{1/2} = 29.8$ s).

³ Gamma rays emitted in the de-excitation of the short-lived daughter ^{137m}Ba ($t_{1/2} = 2.6$ min).

dence on the BU ([Phillips, 1991b](#)) is expected to be valid also in MYRRHA fuel.

Finally, it is often valuable to investigate how the ratio between the densities of some key radionuclides vary as a function of the BU ([Reilly et al., 1991](#)). The advantage of this is that some ratios have been found to be very good indicators of BU ([Reilly et al., 1991](#)). Also, studying the radionuclide ratio instead of the counts of a single radionuclide makes the analysis less sensitive to the measurement geometry (one only has to correct for the energy dependency of the detector efficiency) ([Reilly et al., 1991](#)). Finally, the ¹⁵⁴Eu/¹³⁴Cs ratio has been suggested for discriminating between UO₂ and MOX LWR fuel ([Willman, 2006](#)). There are also more complex ratios that could be studied, for example double ratios involving ¹⁰⁶Ru, ¹³⁴Cs and ¹³⁷Cs ([Nakahara et al., 2000](#); [Dennis and Usman, 2010](#)). However, the lower gamma-ray emission rates from e.g. ¹³⁴Cs in MYRRHA fuel means that even longer measurement times would be required to achieve sufficient accuracy on these more complex ratios. Therefore, we have not included them here. [Fig. 6b](#) shows selected ratios for the MYRRHA fuel and the PWR fuels. It is worth noting that two ratios often suggested, ¹³⁴Cs/¹³⁷Cs and ¹⁵⁴Eu/¹³⁷Cs ([Phillips, 1991b](#)), show a much smaller dependence on BU in MYRRHA than in the PWR cases. On the other hand, the saturation of the ¹⁵⁴Eu/¹³⁷Cs ratio at higher BU in the PWR fuels does not appear as clearly in the MYRRHA case. One of the main reasons for this saturation in PWR fuel is neutron capture by ¹⁵⁴Eu ([Hu et al., 2014](#)), which has a larger capture cross section than ¹⁵³Eu at thermal energies ([Plompen et al., 2020](#)). The capture cross sections for these two isotopes are more similar at fast neu-

tron energies, affecting the balance between ¹⁵⁴Eu production and loss in MYRRHA fuel. This results in a more linear BU-dependence of ¹⁵⁴Eu/¹³⁷Cs in MYRRHA fuel, which could prove useful for determining the BU if sufficient measurement accuracy can be achieved.

3.2. Neutron emission

3.2.1. Total neutron emission

The main source of neutrons in SNF is the spontaneous fission (SF) of a relatively small number of radionuclides. In addition, neutrons are emitted in (α, n) reactions when α particles from decaying heavy nuclides interact with light nuclei present in the fuel ([Ensslin, 1991](#)). All fuel considered in this work are oxide fuels, and ^{17,18}O(α, n) reactions in the SNF constitute a non-negligible source of neutrons ([Simakov et al., 2017](#)). The output of a Serpent depletion simulation does not include the total neutron-emission rate. However, it includes the number densities of the nuclides present in the fuel, and those were in this work converted to an expected neutron-emission rate from SF and (α, n) in the fuel using neutron-yield data from [Simakov et al. \(2017\)](#) and [Simakov et al. \(2015\)](#). The uncertainties in the SF neutron yields in oxide are generally lower than they are for the (α, n) reactions, where most of the assumed yields have relative uncertainties below 9% ([Simakov et al., 2017](#)). The resulting uncertainties in the estimated neutron-emission rates is a limitation of the present work and would to some extent propagate to the parameter-prediction uncertainties when correlating neutron signals to parameters such as BU and CT.

[Fig. 7a](#) shows the resulting total neutron emission rate in the MYRRHA and PWR SNF assemblies as a function of the CT, for three different BUs. It is evident that the total neutron emission rate in MYRRHA fuel has a different dependence on the BU and CT than PWR fuel. While the total neutron emission rate from PWR SNF is strongly dependent on both BU and CT, both of these dependencies appear to be less clear in the MYRRHA case. [Fig. 7b](#) shows the ratio between the neutron emission rate from (α, n) reactions and the neutron emission rate from SF for MYRRHA and the PWR cases. This ratio is commonly known as α ([Ensslin et al., November 1998](#)), and has some implications for safeguards as discussed below. It is clear the BU- and CT-dependence of this parameter is very different in MYRRHA fuel compared to PWR fuel: in this case, the dependence is stronger in MYRRHA fuel. One exception is the UO₂ fuel at the lowest BU considered, where α is relatively high. The reason for this is that the very strong SF neutron emitter ²⁴⁴Cm builds up rapidly in UO₂ fuel at higher BU, so that (α, n) reactions are relatively important at 20 MWd/kgHM.

3.2.2. Potential for neutron multiplicity counting

Because the total neutron emission rate appears to be a weaker BU indicator in MYRRHA fuel than in PWR fuel, it is worth considering what other neutron signatures could be useful for safeguards verification of MYRRHA fuel. One of the fundamental parameters of the neutron emission from the SNF is α , the ratio between (α, n)

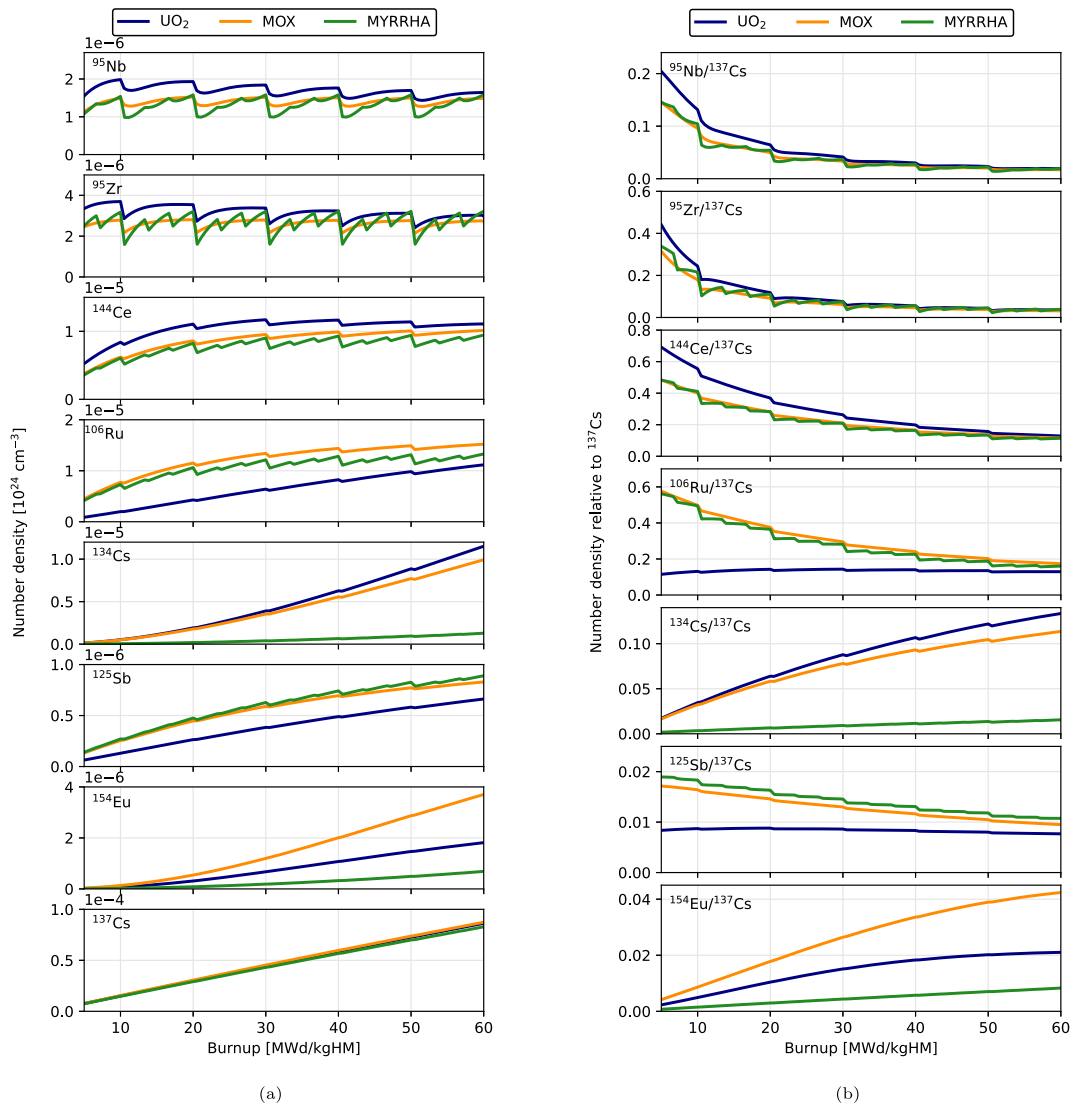


Fig. 6. (a) The number density of the eight fission products important for gamma-ray emission in MYRRHA fuel, as function of burnup. (b) The ratios between the number densities of seven of the fission products and the ¹³⁷Cs number density.

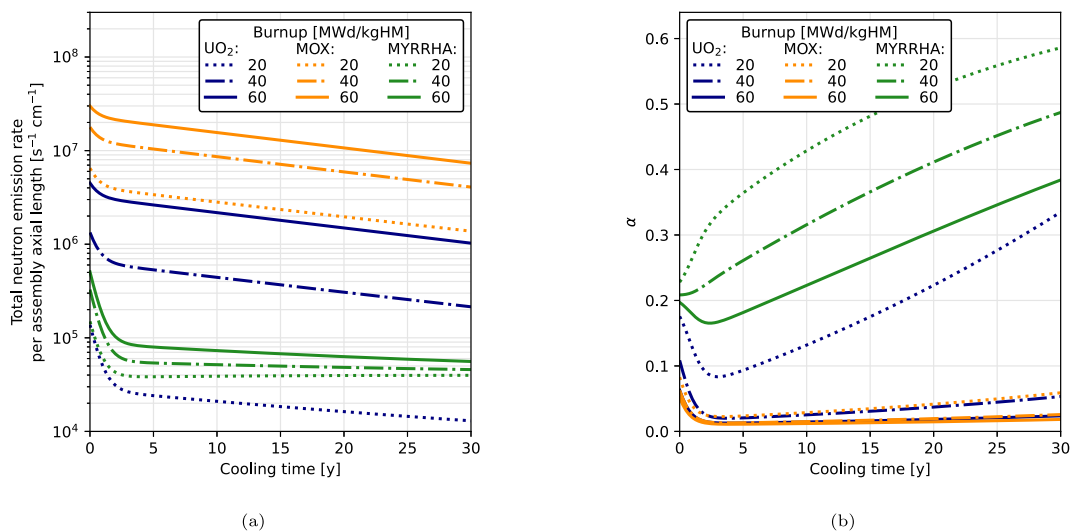


Fig. 7. (a) The axially averaged total neutron emission rate from SF and (α, n) reactions per MYRRHA and PWR FA and (b) the ratio α between the emission rate from (α, n) reactions and the emission rate from SF, as functions of the cooling time after discharge for three different burnups.

and SF emission, and as shown in Fig. 7b this parameter exhibits a relatively strong dependence on BU in MYRRHA SNF. The reason for the stronger BU-dependence of α in MYRRHA fuel compared to PWR fuel is that the combination of the radionuclides contributing to the neutron emission in MYRRHA fuel is more complex than in the PWR fuels. In particular, SF in ^{244}Cm is a dominant neutron source in PWR SNF which is not as important in MYRRHA. This statement is motivated in detail in Section 3.2.3. Because the composition of the neutron source is more complex in the MYRRHA fuel, determining α through NDA measurements of SNF could reveal more information about both BU and CT as well as the composition of the SNF.

The parameter α can be probed experimentally by measuring the time distribution of the neutrons emitted from the SNF: neutrons emitted in a single SF will be time-correlated, while a neutron emitted in an (α, n) reaction is not correlated with any other emitted neutron. Another parameter connected to this time distribution is the neutron multiplicity ν , i. e. the number of neutrons emitted per reaction in the fuel. In (α, n) reactions, only a single neutron is emitted ($\nu = 1$), while for SF ν follows a distribution that is different for different radionuclides. We here consider the average SF multiplicity (ν_{SF}), which is also averaged over the radionuclide content of the SNF. The dependence on BU and CT for MYRRHA and PWR fuel is shown in Fig. 8.

It is evident from Fig. 8 that the SF neutron multiplicity varies more with BU and CT in the MYRRHA SNF than in PWR SNF, again a result of the decreased ^{244}Cm production which completely dominates the neutron emission in PWR SNF. Combined with the stronger dependence of α on BU and CT in MYRRHA fuel, this suggests that measuring the time structure of the neutron emission could prove useful for MYRRHA fuel safeguards as compared to LWR fuel safeguards. Again, it is important to stress that we in this work only consider the emission of radiation in the fuel, and not the radiation transport and/or detection. As is the case for gamma-rays, neutrons can also be scattered and absorbed within the FA or before they reach a detector. In addition, neutron multiplication within the FA will affect the detectable neutron signatures. That is, the neutrons emitted in SF and (α, n) reactions will induce further fissioning in the fuel that affects the neutron rate seen by a detector

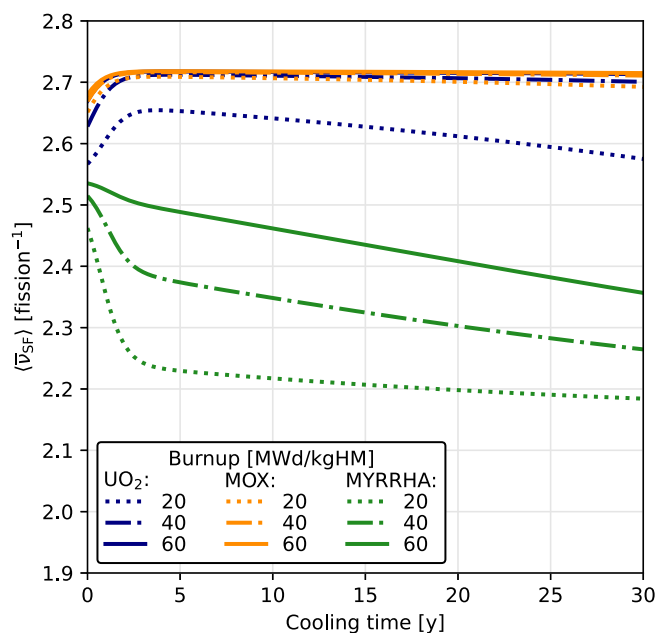


Fig. 8. The average SF multiplicity in MYRRHA and PWR SNF, as functions of burnup and cooling time.

outside the assembly. This self-multiplication can only be taken into account properly by modelling a realistic detector geometry and setup, which is not covered in the present work. All of these effects will have to be taken into account when attempting to measure the neutron signatures discussed above.

3.2.3. Actinide contributions to the neutron emission

The neutron emission from SNF is due to decaying actinides. Fig. 7 shows that the characteristics of the neutron emission in MYRRHA fuel is quite different from the PWR cases, both in terms of the total rate and the relative contributions of SF and (α, n) reactions in the fuel. As was the case for the gamma-ray emission, it is valuable to study the contributions from different radionuclides to the total neutron emission rate to understand these differences. Fig. 9 shows the relative contributions to the total, the SF and the (α, n) neutron emission rates in MYRRHA fuel and the two PWR cases. All radionuclides that contribute at least 1% to the respective rates in MYRRHA fuel are shown explicitly.

As with the radionuclide contributions to the gamma-ray emission rate, some important differences between the contributions to the neutron emission rate from MYRRHA and PWR SNF can be observed. While ^{242}Cm is the main contributor to the neutron emission at CTs of up to one year in all three cases, the contributions to the emission in longer-cooled fuel are very different in the MYRRHA case compared to the PWR cases. ^{244}Cm , which has been shown to be responsible for the vast majority of neutrons emitted from LWR SNF at CTs longer than a few years (Reilly et al., 1991), contributes much less to the neutron emission in MYRRHA SNF than in PWR SNF. As was the case for several of the fission products important for gamma-ray emission (discussed in Section 3.1.4), this is due to the cross sections for neutron capture typically being lower in the fast neutron energy spectrum in MYRRHA compared to the thermal spectrum in a PWR. This reduces the production of ^{244}Cm in MYRRHA fuel.

With a lower content of ^{244}Cm in the SNF, neutron emissions from the plutonium isotopes contributes relatively more to the neutron emission rate in MYRRHA fuel. This means that measuring the properties of the neutron emission from MYRRHA fuel could provide a more direct access to the plutonium content of the fuel than would measuring ^{244}Cm (which can only be said to be a “proxy” of the plutonium content). The plutonium isotopes with even mass number (238, 240 and 242) have considerable SF rates (Simakov et al., 2015), but as shown in Fig. 9b only ^{240}Pu and ^{242}Pu contribute to the SF neutron emission rate due to their abundance in the MYRRHA fuel. For neutrons from (α, n) reactions, the lower ^{244}Cm content again increases the relative importance of the plutonium isotopes, as shown in Fig. 9c. In addition, ^{241}Am is a very important (α, n) source, especially at longer CTs. The neutron emission from SF and (α, n) reactions in a MYRRHA assembly with a BU of 60 MWd/kgHM is detailed in Tables 6 and 7.

3.2.4. BU-dependence of the total neutron emission

The fact that ^{244}Cm is less dominant in the neutron emission in MYRRHA SNF than it is in LWR SNF can have several interesting implications for safeguards, since well-established assumptions about the characteristics and BU-dependence of the neutron emission from LWR SNF may not hold true for MYRRHA SNF. The composition of the neutron source becomes more complex as a larger number of radionuclides have substantial contributions to the total neutron emission. To illustrate the potential consequences for the analysis of NDA measurements of SNF, Fig. 10 shows the total neutron emission rate after a CT of five years as a function of BU in MYRRHA and the PWR cases. The CT was chosen such that much of the ^{242}Cm , with a half-life of 163 days, had decayed and thus contributes very little to the total neutron emission. Here, the contribution from SF in ^{244}Cm is shown explicitly, and it is evident that

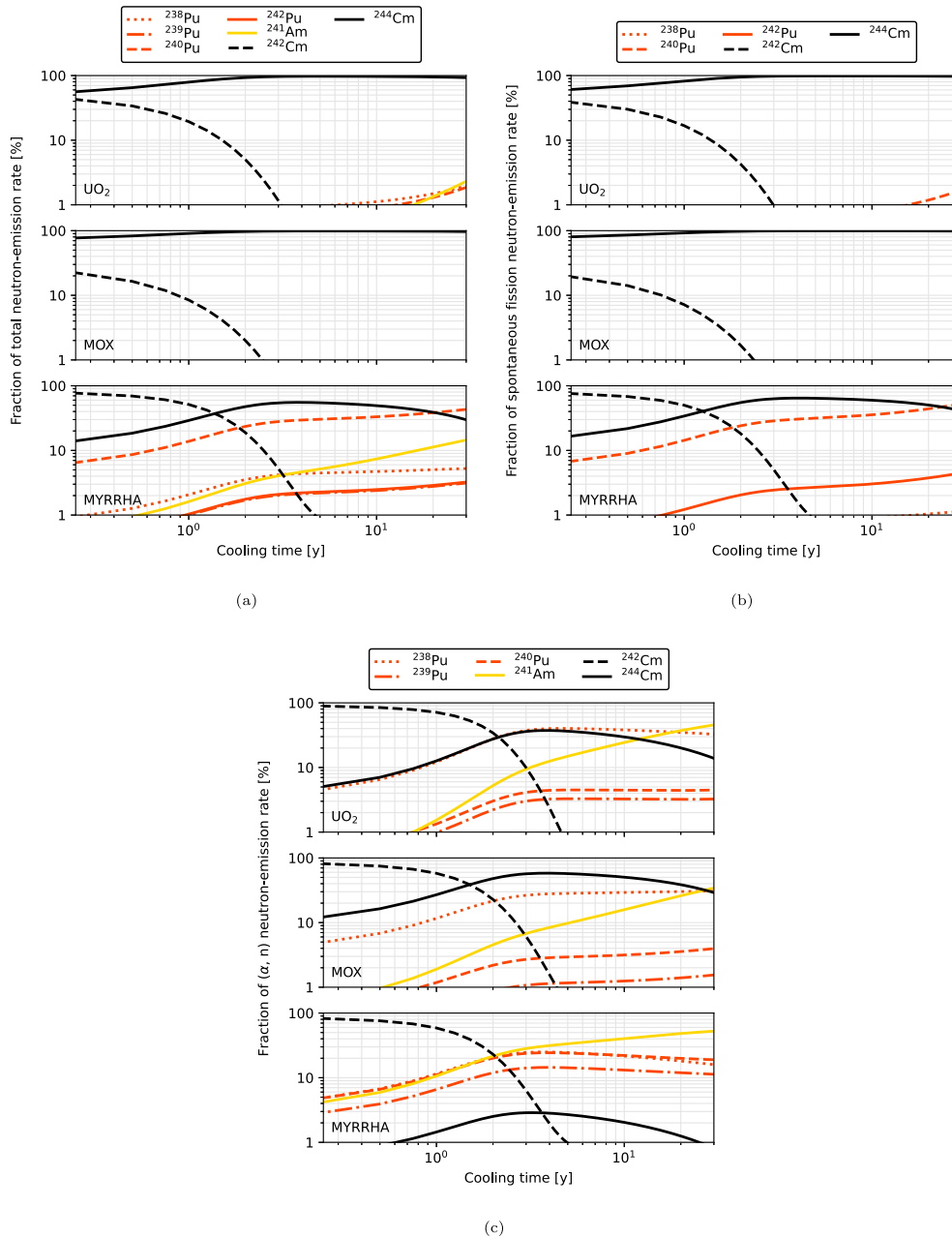


Fig. 9. The relative contributions from important radionuclides to the neutron emission rate from (a) both SF and (α, n) reactions, (b) only SF and (c) only (α, n) reactions in the PWR UO₂ and MOX cases (both at a discharge burnup of 40 MWd/kgHM) and MYRRHA (at a discharge burnup of 60 MWd/kgHM) as functions of the cooling time after discharge.

Table 6

Radionuclide contributions to the SF neutron emission rate in a MYRRHA FA with a discharge burnup of 60 MWd/kgHM. Only rates at cooling times below 20 nuclide half lives are shown.

Cooling time [y]	Spontaneous fission neutron emission rate per assembly axial length [$10^3 \text{ s}^{-1} \text{ cm}^{-1}$]					
	²³⁸ Pu	²⁴⁰ Pu	²⁴² Pu	²⁴² Cm	²⁴⁴ Cm	Others
1	0.57	21	1.8	74	50	$4.2 \cdot 10^{-3}$
5	0.56	21	1.8	0.57	43	$4.8 \cdot 10^{-3}$
10	0.54	21	1.8	-	36	$5.3 \cdot 10^{-3}$
20	0.50	21	1.8	-	24	$6.0 \cdot 10^{-3}$
30	0.46	21	1.8	-	17	$6.4 \cdot 10^{-3}$

Table 7

Radionuclide contributions to the (α, n) neutron emission rate in a MYRRHA FA with a discharge burnup of 60 MWd/kgHM. Only rates at cooling times below 20 nuclide half lives are shown.

Cooling time [y]	(α, n) neutron emission rate per assembly axial length [$10^3 \text{ s}^{-1} \text{ cm}^{-1}$]						Others
	^{238}Pu	^{239}Pu	^{240}Pu	^{241}Am	^{242}Cm	^{244}Cm	
1	3.0	1.7	2.9	2.8	16	0.38	$5.8 \cdot 10^{-3}$
5	3.0	1.7	2.9	4.1	0.12	0.33	$5.3 \cdot 10^{-3}$
10	2.9	1.7	2.9	5.4	-	0.27	$4.7 \cdot 10^{-3}$
20	2.7	1.7	2.9	7.1	-	0.18	$3.9 \cdot 10^{-3}$
30	2.5	1.7	2.9	8.1	-	0.13	$3.4 \cdot 10^{-3}$

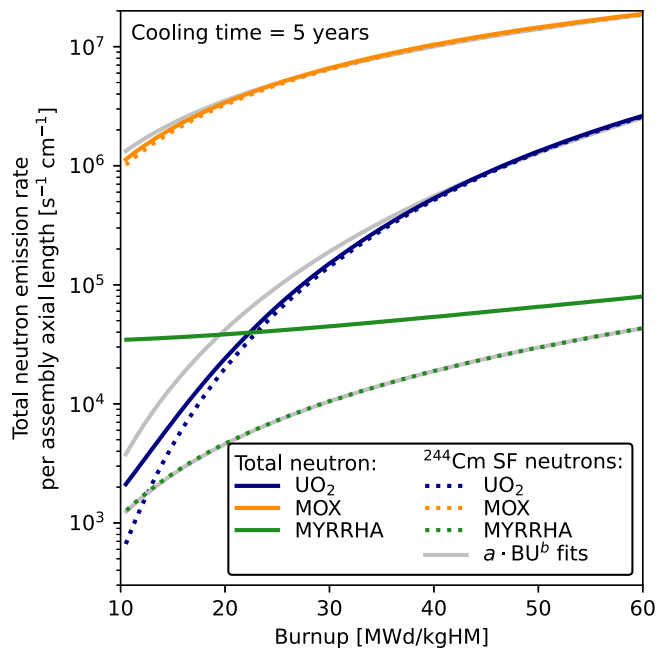


Fig. 10. The total neutron emission rate from five-year cooled MYRRHA and PWR SNF assemblies as a function of burnup.

the decreased production of this radionuclide in MYRRHA has a direct effect on the BU-dependence of the total neutron emission. In both of the PWR cases, SF in ^{244}Cm is the major source of emitted neutrons and practically determines the total neutron emission rate.

The total neutron emission rate from SNF is commonly used as an indicator of the fuel BU, and is therefore useful in safeguards inspections. For LWR SNF, an NDA measurement of the total emission from SNF can be used to determine the contribution from ^{244}Cm , which is directly related to BU (Rinard et al., 1988). It has been found that for LWR UO_2 fuel, the total neutron emission rate is related to BU via a power-law relationship (Rinard et al., 1988; Reilly et al., 1991):

$$\text{Neutron emission rate} = a \cdot \text{BU}^b, \quad (1)$$

which has been found to be valid above a BU of approximately 10 MWd/kgHM. The parameter a in Eq. 1 is a scaling factor that depends on the initial composition of the fuel, and it has been found that the fit parameter b is often between 3 and 4 for LWR UO_2 fuels (Reilly et al., 1991). Because ^{244}Cm is so important for the total neutron emission from LWR SNF, Eq. 1 is fundamentally related to the build-up of ^{244}Cm . To determine the power-law dependence of the ^{244}Cm SF neutron emission rate on BU for MYRRHA SNF, Eq. 1 was fitted to the ^{244}Cm SF neutron emission rates shown in Fig. 10. The values of the fit parameters a and b are shown in Table 8.

Table 8

Values of the fit parameters a and b when fitting the power law $a \cdot \text{BU}^b$ to the burnup-dependent ^{244}Cm SF neutron emission rate from MYRRHA and PWR SNF. The quality of the fits is given by the coefficient of determination R^2 .

Fuel	a	b	R^2
PWR- UO_2	0.58 ± 0.04	3.73 ± 0.02	0.9991
PWR-MOX	$(3.80 \pm 0.09) \cdot 10^4$	1.511 ± 0.006	0.9990
MYRRHA	10.24 ± 0.06	2.038 ± 0.001	0.9999

Several things of interest can be seen in Table 8 – first between the PWR UO_2 and PWR MOX, and also between both of them and the MYRRHA fuel. For the UO_2 fuel, the value of b is within the expected range for UO_2 fuel (i. e. between 3 and 4), while for PWR MOX it is significantly smaller. For MYRRHA, b lies between the PWR values, meaning that the BU-dependence of the ^{244}Cm production in MYRRHA fuel lies between the PWR cases. In addition, the total neutron emission in MYRRHA fuel can no longer be said to be well described by only the ^{244}Cm emission. This is evident from both Fig. 10 and Fig. 9. Therefore, describing the BU-dependence of the total neutron emission by a simple power law is no longer appropriate for MYRRHA fuel, as is clear from the reduced quality of the fit in Table 8. Additionally, the BU-dependence of the total neutron emission is not as strong in MYRRHA fuel as in PWR fuel, as was also clear from Fig. 7a.

3.2.5. Actinide inventory

As shown in the previous sections, the neutron emission in MYRRHA SNF differs in many ways from that in PWR SNF. With respect to the build-up of the important neutron-emitting actinides in MYRRHA fuel during irradiation (as studied for the gamma-emitting fission products in Section 3.1.4), Fig. 11 shows the actinide number densities (the number of nuclei per cm^3) as functions of burnup in MYRRHA and PWR fuel, obtained from Serpent simulations.

In Fig. 11, it is clear that plutonium content in the MYRRHA fuel decreases with BU, which is similar to the PWR MOX case (although the total plutonium content is higher in MYRRHA) due to fissioning of plutonium. The build-up of ^{241}Am with BU in MYRRHA fuel is higher than in UO_2 fuel because ^{241}Am is readily produced in β^- decay of ^{241}Pu which is present already in the fresh MYRRHA fuel. This is also the reason why the build-up is higher in PWR MOX fuel than PWR UO_2 . In addition, the neutron-capture $^{241}\text{Am}(n, \gamma)^{242}\text{Am}$ reaction is less likely in the fast neutron energy spectrum in MYRRHA. As a result, the net build-up of ^{241}Am is greater in MYRRHA than in PWR MOX fuel. An additional effect of this can be seen when considering the build-up of ^{242}Cm , which is produced in the β^- decay of ^{242}Am . From Fig. 11, it is clear that the build-up of ^{242}Cm is lower in MYRRHA fuel than in the PWR-MOX case, as a direct effect of the lower capture cross section of ^{241}Am at fast neutron energies. The ^{242}Cm is however larger than in UO_2 fuel because of the higher initial plutonium content in the fuel.

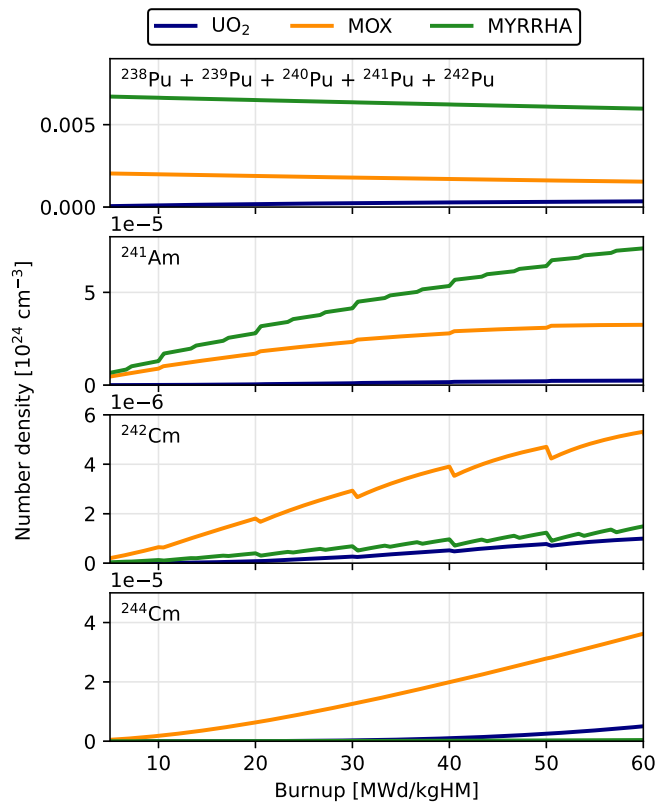


Fig. 11. The number density of the actinides important for neutron emission in MYRRHA fuel, as function of burnup.

Perhaps the most striking difference between the actinide build-up in MYRRHA and the PWR cases can be seen for ^{244}Cm , where the build-up is very much lower than in both of the PWR cases. This can be understood by studying the actinide transmutation paths in the fuel. Production of ^{244}Cm first requires production of the plutonium isotopes (Sasahara et al., 2008). In PWR UO₂ fuel, these are produced mainly through neutron captures in a chain starting with ^{238}U (Hsue et al., 1979; Schillebeeckx et al., 2020). Nonetheless, for UO₂ there are a number of nuclides not present in the fresh fuel that first must be produced to initiate ^{244}Cm production, which explains the high dependence on BU (which is proportional to the neutron fluence rate). In PWR MOX fuel, the plutonium isotopes are already present in fresh fuel, and fewer steps in the transmutation chain are needed to produce ^{244}Cm . This results in a lower dependence on BU than in the PWR UO₂ case. For MYRRHA, the plutonium isotopes are also present in the fresh fuel. However, due to the fast neutron energy spectrum, the fission-to-capture ratio is generally higher for the actinides than in a PWR core (Plompen et al., 2020). The effect is the same as for the fission products discussed in Section 3.1.4: production paths requiring neutron capture are suppressed in MYRRHA compared to the PWR cases. As discussed above, this has implications for safeguards verification since the neutron emission in SNF is typically assumed to come almost entirely from SF in ^{244}Cm . The reason for the much lower build-up in MYRRHA fuel is (again) the lower neutron-capture cross sections for fast neutrons. The production of ^{244}Cm requires a number of neutron captures by actinides in the fuel (Reilly et al., 1991), and is therefore decreased in MYRRHA. Additionally, the fission-to-capture ratio in several of the actinides increases in a fast spectrum (Plompen et al., 2020), so that the transmutation path needed for ^{244}Cm production is more frequently aborted through fission. The main difference between the build-up of ^{242}Cm and ^{244}Cm is therefore the larger number

of subsequent captures needed to form ^{244}Cm from the plutonium isotopes in the fuel.

4. Discussion

There are several examples of operating, decommissioned or planned fast reactors using HEU or MOX with a high IPC as fuel (Tsvetkov et al., 2012), and in that respect MYRRHA is not unique. The results presented in this paper can therefore be of relevance in the more general context of fast reactor safeguards, although the particular operational characteristics might be different from MYRRHA. Due to the renewed interest in developing fast reactors, this is of special relevance today. Safeguards measures for future facilities should also be developed to handle more practical issues that are not encountered in today's inspection of LWR fuel. For example, the increased corrosion risk when using LBE as coolant as in MYRRHA (Weisenburger et al., 2011) could affect the choice of SNF storage. Should the SNF be submerged in LBE (instead of water) after discharge from the core, direct visual inspection will not be possible. This would also have implications for what radiation signatures could be measured as well as how.

The fact that the characteristics of the radiation emitted from MYRRHA SNF are considerably different from the radiation emitted from PWR SNF will impact the choice of NDA instruments as well as the NDA analysis methods. Radiation transport from the FA to, and detection by, an NDA instrument is not covered in the present work, but it is clear that the measurement conditions will have an additional effect on the detectable radiation due to scattering, attenuation and self-multiplication. The design of the SNF storage in MYRRHA is not yet defined, but if also the SNF will be stored in LBE, this will affect the radiation transport and consequently the choice of NDA instrumentation: if the SNF is stored in LBE, neutron-based techniques are likely to be more relevant due to the high gamma-ray attenuation. There are additional sources of uncertainty in the results presented here: first, a constant power level (i. e. independent of irradiation cycle) in an infinite lattice has been assumed. The actual power and geometry variations in the core will have an impact on the radionuclide inventory in a single FA. The extent to which determination of IE, BU and CT using NDA is sensitive to the power variations is the topic of ongoing research (Branger et al., 2021). Second, there are uncertainties associated with the nuclear data and in the depletion calculation. These uncertainties will be different for different radionuclides – for instance the ^{154}Eu build-up depends on a large number of predecessors and so will be sensitive to variations in cross sections and fission yields. An uncertainty of ~14% in the ^{154}Eu number density at a BU of 40 MWd/kgHM in a PWR has been reported (Rochman and Sciolla, 2014), with uncertainties typically lower for nuclides with less complex production paths. These uncertainties will also to some extent depend on the neutron energy spectrum. These effects can be accounted for in future work, but it is nonetheless possible to make some general remarks on the detection of radiation from the MYRRHA SNF. In this discussion, we limit ourselves to passive NDA measurements (i. e. only relying on the radiation emitted from the SNF itself).

Concerning gamma NDA measurements, Fig. 3 shows that the BU-dependence of the total gamma-ray emission rate above 500 keV is similar in MYRRHA SNF as in the PWR fuels. Therefore, measuring the total gamma rate could serve as an important tool for determining a range of possible IPC, BU and CT values for the assayed FA. The relative contributions from ^{134}Cs and ^{154}Eu to the total gamma-ray emission rate is lower in MYRRHA SNF than in the PWR SNF. This means that if an identical NDA setup would be used to assay MYRRHA and PWR SNF, a longer measurement time would be needed for the MYRRHA measurement to measure

the intensities of the ^{134}Cs and ^{154}Eu emissions with the same statistical accuracy. This could also make measurements of radionuclide ratios involving these nuclides less feasible in MYRRHA. When considering the more short-lived gamma-ray emitters, ^{106}Ru has a relatively high build-up in the MYRRHA fuel and also emits gamma rays with relatively high energies (see Table 5), which are therefore relatively penetrating in the FA and surrounding material. These properties could make spectroscopic measurements of ^{106}Ru gamma rays useful at a CT shorter than approximately eight years. In general, the usefulness of gamma spectroscopy as a tool for NDA of MYRRHA SNF will improve at short CT, where several radionuclides could provide complementary information about IPC, BU and CT. This means that it would be advantageous to have access to the SNF relatively soon after discharge from the core. A practical consideration that could influence the measurement of fission products in SNF is their migration in the fuel (Phillips et al., 1980). It has been shown (Phillips et al., 1979) that this effect can be especially severe in fast reactors due to the high fuel-temperature gradients, although it is not yet clear how large this effect could be in MYRRHA fuel. Finally, direct measurements of plutonium via gamma-spectroscopy (e. g. on the 375-keV line, as shown in Fig. 4) appears to be more feasible in MYRRHA although further work is needed to study the effects of gamma-ray scattering and attenuation in a measurement situation.

For neutron NDA measurements, Fig. 7a shows that the BU- and CT-dependence of the total neutron emission rate is weaker in MYRRHA SNF than in the PWR fuels. As a result, measuring the total neutron rate from MYRRHA SNF is less useful than it is for PWR fuels for verifying these parameters. As shown in Fig. 10, the decreased influence of ^{244}Cm on the total neutron emission rate in MYRRHA fuel means that new analysis techniques should be developed to correlate the total neutron rate with different radionuclide contributions. On the other hand, neutron-detection techniques will be more sensitive to the plutonium content of the MYRRHA SNF. The larger dependence on plutonium in the fast-reactor SNF neutron emission has been noted previously (Persiani and Gundy, 1982; Lestone et al., 2002). In order to identify the contributions from different radionuclides to the neutron emission, NDA techniques based on measurement of the neutron-emission time structure should be considered. As shown in Figs. 7b and 8, parameters connected to the neutron multiplicity have a relatively strong dependence on BU and CT in MYRRHA SNF. Time-dependent measurements of the neutron emission could for example be based on coincidence or multiplicity counting (Ensslin et al., November 1998). Such instruments could also measure the total neutron rate. Neutron-coincidence counting has been used to assay fast-reactor SNF in the past (Lestone et al., 2002), and although simulation studies have shown that the neutron rate from SNF is so high that multiplicity counting is unfeasible (Croft et al., 2011), those studies assumed PWR SNF with most neutrons due to SF in ^{244}Cm . Others have also pointed out that if the plutonium contribution to the neutron emission is comparable to that from curium, neutron-multiplicity measurements could be useful for distinguishing the different neutron sources (Rinard and Menlove, 1996). If the NDA instrument is only sensitive to thermal neutrons, the storage medium of the MYRRHA SNF has an impact: if the SNF is stored in LBE, significant thermalisation will not occur and the NDA instrument would have to be modified. An alternative approach could be based on fast-neutron detection, which has been studied in the context of NDA instrumentation in recent years (Di Fulvio et al., 2017; Shin et al., 2019). Such systems could measure also other characteristics of the neutron field, such as angular correlation. Also, the much faster response of a fast-neutron system compared to a thermal-neutron system reduces the background rate (Chichester et al., 2015), which is crucial for multiplicity measurements.

Based on the above discussions, it is clear that a combination of NDA instruments may be necessary to accurately determine IPC, BU and CT of MYRRHA SNF. This approach has already been suggested for future NDA techniques in nuclear safeguards (Charlton et al., 2012). The results of this paper indicate that NDA techniques based on neutron detection could be more useful than those based on gamma detection for MYRRHA safeguards, although the complementary nature of a total gamma measurement would add information about the SNF properties. It should also be pointed out that we in this paper only consider one specific IPC in the fuel (30%), and one specific isotopic mix of plutonium. Others have highlighted the special need for complementary techniques when assaying MOX fuel due to the additional complexity added by the plutonium-vector composition (Bolind, 2014). Therefore, it is more reasonable to attempt to assay more specific quantities than the IPC, such as fissile mass or plutonium mass and isotopic composition in the MYRRHA SNF.

5. Conclusion and outlook

In this study, we have presented results from depletion simulations of fuel in the LBE-cooled fast reactor MYRRHA to understand the requirements on future NDA instrumentation for MYRRHA safeguards. The results show how the gamma-ray and neutron emission in a SNF assembly depends on BU and CT, and how the relevant radionuclides build up in the SNF. The results are systematically compared to simulation results for PWR UO_2 and MOX fuels, and demonstrate that there are considerable and important differences in the characteristics of the gamma-ray and neutron emission in MYRRHA SNF compared to PWR SNF, both with regards to intensity, energy and contributing radionuclides. The main differences are due to the fast neutron energy spectrum in MYRRHA, which reduces the production rates of several radionuclides relevant in safeguards NDA, such as ^{134}Cs , ^{154}Eu and ^{244}Cm . As a result, the potential for gamma-spectroscopic measurements at long CT is lower for MYRRHA fuel than for PWR fuels, and the neutron emission is to a larger extent due to SF in plutonium. As a result, NDA techniques that are currently adopted for verification of LWR SNF may not be well suited for verification of MYRRHA SNF. Key topics for further research are how scattering, attenuation and self-multiplication in the measurement setup affect the radiation signatures from the SNF, the impact of the IPC and initial plutonium vector, the possibilities for using neutron-based NDA techniques to assay the plutonium composition of the SNF, as well as modelling of NDA instrumentation and detection of the emitted radiation.

CRediT authorship contribution statement

M. Preston: Conceptualization, Formal analysis, Investigation, Methodology, Software, Writing - original draft. **A. Borella:** Conceptualization, Methodology, Writing - review & editing. **E. Branger:** Conceptualization, Methodology, Writing - review & editing. **S. Grape:** Conceptualization, Methodology, Writing - review & editing. **R. Rossa:** Conceptualization, Methodology, Writing - review & editing.

Declaration of Competing Interest

The authors declare that they have no known competing financial interests or personal relationships that could have appeared to influence the work reported in this paper.

Acknowledgements

This work was funded by the Swedish Research Council (project ID 2019-04577).

References

- Ait Abderrahim, H., Sobolev, V., Malambu, E., 2005. Fuel design for the experimental ADS MYRRHA. In: Technical Meeting on use of LEU in ADS, International Atomic Energy Agency, Vienna, Austria. .
- Ait Abderrahim, H., Baeten, P., De Bruyn, D., Fernandez, R., 2012. MYRRHA – A multi-purpose fast spectrum research reactor. *Energy Convers. Manag.* 63, 4–10. <https://doi.org/10.1016/j.enconman.2012.02.025>.
- Barnes, B.K., Phillips, J.R., Waterbury, G.R., Quintana, J.N., Netuschil, J.R., Murray, A. S., 1979. Characterization of irradiated nuclear fuels by precision gamma scanning. *J. Nucl. Mater.* 81, 177–184. [https://doi.org/10.1016/0022-3115\(79\)90076-X](https://doi.org/10.1016/0022-3115(79)90076-X).
- Baron, D., Hallstadius, L., Kulacsy, K., Largenton, R., Noiro, J., 2020. Fuel Performance of Light Water Reactors (Uranium Oxide and MOX), in: R.J.M. Konings, R.E. Stoller, J. Noiro (Eds.), *Comprehensive Nuclear Materials*, 2nd Edition, Vol. 2, Elsevier, Amsterdam, the Netherlands. Ch. 2, p. 42. doi: 10.1016/B978-0-12-803581-8.11707-2. .
- Bathke, C.G., Ebbinghaus, B.B., Collins, B.A., Sleaford, B.W., Hase, K.R., Robel, M., Wallace, R.K., Bradley, K.S., Ireland, J.R., Jarvinen, G.D., Johnson, M.W., Prichard, A.W., Smith, B.W., 2011. The Attractiveness of Materials in Advanced Nuclear Fuel Cycles for Various Proliferation and Theft Scenarios. *Nucl. Technol.* 179, 5–30. <https://doi.org/10.13182/NT10-203>.
- Bolind, A.M., 2014. The use of the BIC set in the characterization of used nuclear fuel assemblies by nondestructive assay. *Ann. Nucl. Energy* 66, 31–50. <https://doi.org/10.1016/j.anucene.2013.11.010>.
- Branger, E., Elter, Zs., Grape, S., Preston, M., 2021. Investigating the sensitivity to irradiation history when predicting fuel parameters using random forest regression. *ESARDA Bull.* 62, in press.
- Charlton, W.S., Humphrey, M.A., 2012. External Review of the Next Generation Safeguards Initiative's Spent Fuel Nondestructive Assay Project. *J. Nucl. Mater. Manag.* 40 (3), 12–17.
- Chichester, D.L., Thompson, S.J., Kinlaw, M.T., Johnson, J.T., Dolan, J.L., Flaska, M., Pozzi, S.A., 2015. Statistical estimation of the performance of a fast-neutron multiplicity system for nuclear material accountability. *Nucl. Instrum. Meth. A* 784, 448–454. <https://doi.org/10.1016/j.nima.2014.09.027>.
- Chirayath, S.S., Osborn, J.M., Coles, T.M., 2018. Trace Fission Product Ratios for Nuclear Forensics Attribution of Weapons-Grade Plutonium from Fast and Thermal Reactors. *Sci. Glob. Secur.* 23 (1), 48–67. <https://doi.org/10.1080/08929882.2015.996079>.
- Croft, S., Evans, L.G., Scheer, M., Swinhoe, M.T., et al., 2011. Feasibility of Classic Multiplicity Analysis Applied to Spent Nuclear Fuel Assemblies, Tech. Rep. LA-UR-11-00512, Los Alamos National Laboratory, Los Alamos, NM, USA. .
- Dennis, M.L., Usman, S., 2010. Feasibility of ^{106}Ru peak measurement for MOX fuel burnup analysis. *Nucl. Eng. Des.* 240(10). doi: 10.1016/j.nucengdes.2010.07.003. .
- Di Fulvio, A., Shin, T.H., Jordan, T., Sosa, C., Ruch, M.L., Clarke, S.D., Chichester, D.L., Pozzi, S.A., 2017. Passive assay of plutonium metal plates using a fast-neutron multiplicity counter. *Nucl. Instrum. Meth. A* 855, 92–101. <https://doi.org/10.1016/j.nima.2017.02.082>.
- Di Maria, S., Ottolini, M., Malambu Mbala, E., Sarotto, M., Castellini, D., 2012. Neutronic characterization and decay heat calculations in the in-vessel fuel storage facilities for MYRRHA/FASTEF, *Energy Convers. Manag.* 64, 522–529. <https://doi.org/10.1016/j.enconman.2012.05.001>.
- Durst, P.C., Therios, I., Bean, R., Dougan, A., Boyer, B., Wallace, R.L., Ehinger, M.H., Kovacic, D.N., Tolk, K., 2007. Advanced Safeguards Approaches For New Fast Reactors, Tech. Rep. PNNL-17168, Pacific Northwest National Laboratory, Richland, WA, USA. .
- Elter, Zs., Pöder Balke, L., Branger, E., Grape, S., 2020. Pressurized water reactor spent nuclear fuel data library produced with the Serpent2 code. *Data Brief* 33, 106429. <https://doi.org/10.1016/j.dib.2020.106429>.
- Ensslin, N., 1991. The Origin of Neutron Radiation. In: D. Reilly, N. Ensslin, H. Smith, Jr. (Eds.), *Passive Nondestructive Assay of Nuclear Materials*, Office of Nuclear Regulatory Research, Washington, DC, USA, Ch. 11. .
- Ensslin, N., Harker, W.C., Krick, M.S., Langner, D.G., Pickrell, M.M., Stewart, J.E., 1998. Application Guide to Neutron Multiplicity Counting, Tech. Rep. LA-13422-M, Los Alamos National Laboratory, Los Alamos, NM, USA. .
- Galloway, J.D., Trelue, H.R., Fensin, M.L., Broadhead, B.L., 2012. Design and Description of the NGS Spent Fuel Library with Emphasis on the Passive Gamma Signal. *J. Nucl. Mater. Manag.* 40 (3), 25–35.
- Gelineau, O., Gavrilov, S., 2012. Final report material property requirements for ASTRID and MYRRHA ADS system (Tech. rep.). Matter – Seventh Framework Programme. .
- Grape, S., Jacobsson Svård, S., Hellesen, C., Jansson, P., Åberg Lindell, M., 2014. New perspectives on nuclear power—Generation IV nuclear energy systems to strengthen nuclear non-proliferation and support nuclear disarmament. *Energy Policy* 73, 815–819. <https://doi.org/10.1016/j.enpol.2014.06.026>.
- Håkansson, A., Bäcklin, A., 1995. Non-destructive Assay of Spent BWR Fuel with High-resolution Gamma-ray Spectroscopy (Tech. Rep. 95:19). Statens Kärnkraftinspektion, Stockholm, Sweden. .
- Henzl, V., 2014. Evaluation of Differential Die-Away Technique Potential in Context of Non-Destructive Assay of Spent Nuclear Fuel, Tech. Rep. LA-UR-14-29224. Los Alamos National Laboratory, Los Alamos, NM, USA. .
- Hsue, S.T., Crane, T.W., Colbert, W.L., Jr., Lee, J.C., 1978. Nondestructive assay methods for irradiated nuclear fuels, Tech. Rep. LA-6923, Los Alamos National Laboratory, Los Alamos, NM, USA. .
- Hsue, S.T., Stewart, J.E., Kaieda, K., Halbig, J.K., Phillips, J.R., Lee, D.M., Hatcher, C.R., 1979. Passive Neutron Assay of Irradiated Fuels (Tech. Rep. LA-7645-MS). Los Alamos National Laboratory, Los Alamos, NM, USA. .
- Hu, J., Gauld, I.C., Banfield, J.E., Skutnik, S.E., 2014. Developing Spent Fuel Assembly Standards for Advanced NDA Instrument Calibration – NGS Spent Fuel Project, Tech. Rep. ORNL/TM-2013/576, Oak Ridge National Laboratory, Oak Ridge, TN, USA. .
- International Atomic Energy Agency, 1992. Determination of Research Reactor Fuel Burnup, no. IAEA-TECDOC-633, IAEA, Vienna, Austria. .
- International Atomic Energy Agency, 2001. IAEA Safeguards, 2001 Edition, no. 3 in International Nuclear Verification Series, IAEA, Vienna, Austria. .
- International Atomic Energy Agency, 2011. Safeguards Techniques and Equipment: 2011 Edition, 2nd Edition, no. 1 in International Nuclear Verification Series, IAEA, Vienna, Austria. .
- Jaluvka, D., 2015. Development of a Core Management Tool for the MYRRHA Irradiation Research Facility, Ph.D. thesis, KUL – Katholieke Universiteit Leuven, Leuven, Belgium. .
- Jansson, P., 2002. Studies of Nuclear Fuel by Means of Nuclear Spectroscopic Methods (Ph.D. thesis). Uppsala Universitet, Uppsala, Sweden. .
- Kennedy, G., Van Tichelen, K., Pacio, J., Di Piazza, I., Uitslag-Doolaar, H., 2020. Thermal-Hydraulic Experimental Testing of the MYRRHA Wire-Wrapped Fuel Assembly. *Nucl. Technol.* 206, 179–190. <https://doi.org/10.1080/00295450.2019.1620539>.
- Leppänen, J., Pusa, M., Viitanen, T., Valtavirta, V., Kältiäinenaho, T., 2013. The Serpent Monte Carlo code: Status, development and applications in 2013. *Ann. Nucl. Energy* 82, 142–150. <https://doi.org/10.1016/j.anucene.2014.08.024>.
- Lestone, J.P., Pecos, J.M., Rennie, J.A., Sprinkle Jr., J.K., Staples, P., Grimm, K.N., Hill, R. N., Cherradi, I., Islam, N., Koulikov, J., Starovich, Z., 2002. The passive nondestructive assay of the plutonium content of spent-fuel assemblies from the BN-350 fast-breeder reactor in the city of Aqtou, Kazakhstan. *Nucl. Instrum. Meth. A* 490, 409–425. [https://doi.org/10.1016/S0168-9002\(02\)00912-9](https://doi.org/10.1016/S0168-9002(02)00912-9).
- Locatelli, G., Mancini, M., Todeschini, N., 2013. Generation IV nuclear reactors: Current status and future prospects. *Energy Policy* 61, 1503–1520. <https://doi.org/10.1016/j.enpol.2013.06.101>.
- Mueller, A.C., 2013. Transmutation of Nuclear Waste and the future MYRRHA Demonstrator. *J. Phys.: Conf. Ser.* 420. <https://doi.org/10.1088/1742-6596/420/1/012059>.
- Nakahara, Y., Suyama, K., Suzuki, T., 2000. Technical development on burn-up credit for spent LWR fuels (Tech. Rep. 2000–071). Japan Atomic Energy Research Institute, Tokai, Ibaraki, Japan. .
- Nondestructive Assay of SEFOR Fuel Rods, 1969. Los Alamos National Laboratory Program Status Report April-June 1969, Tech. Rep. LA-4227-MS, Los Alamos National Laboratory, USA. .
- Neutron Self-Indication Assay of SEFOR Fuel Rods, 1969. Los Alamos National Laboratory Program Status Report July-September 1969, Tech. Rep. LA-4315-MS, Los Alamos National Laboratory, USA. .
- Osborn, J.M., 2018. Nuclear Forensics Methodology for Source Reactor-Type Discrimination of Chemically Separated Plutonium, Ph.D. thesis, Texas A&M University, College Station, TX, USA. .
- Persiani, P.J., Gundy, M.L., 1982. NDA Safeguards Techniques for LMFBR Assemblies, Tech. Rep. ANL-82-49. Argonne National Laboratory, Argonne, IL, USA. .
- Phillips, J.R., 1991. Irradiated Fuel Measurements. In: D. Reilly, N. Ensslin, H. Smith, Jr. (Eds.), *Passive Nondestructive Assay of Nuclear Materials*, Office of Nuclear Regulatory Research, Washington, DC, USA, Ch. 18. .
- Phillips, J.R., 1991. Irradiated Fuel Measurements. In: D. Reilly, N. Ensslin, H. Smith, Jr. (Eds.), *Passive Nondestructive Assay of Nuclear Materials*, Office of Nuclear Regulatory Research, Washington, DC, USA, Ch. 18, p. 534. .
- Phillips, J.R., 1991. Irradiated Fuel Measurements. In: D. Reilly, N. Ensslin, H. Smith, Jr. (Eds.), *Passive Nondestructive Assay of Nuclear Materials*, Office of Nuclear Regulatory Research, Washington, DC, USA, Ch. 18, p. 540. .
- Phillips, J.R., 1991. Irradiated Fuel Measurements, in: D. Reilly, N. Ensslin, H. Smith, Jr. (Eds.), *Passive Nondestructive Assay of Nuclear Materials*, Office of Nuclear Regulatory Research, Washington, DC, USA, Ch. 18, pp. 540–541. .
- Phillips, J.R., Barnes, B.K., Bement, T.R., 1979. Correlation of the Cesium-134/Cesium-137 Ratio to Fast Reactor Burnup. *Nucl. Technol.* 46, 21–29. doi: <https://doi.org/10.13182/NT46-21>.
- Phillips, J.R., Halbig, J.K., Lee, D.M., Beach, S.E., Bement, T.R., Dermendjiev, E., Hatcher, C.R., Kaieda, K., Medina, E.G., 1980. Application of Nondestructive Gamma-Ray and Neutron Techniques for the Safeguarding of Irradiated Fuel Materials, Tech. Rep. LA-8212, Los Alamos National Laboratory, Los Alamos, NM, USA. .
- Plompen, A.J.M., Cabellos, O., De Saint Jean, C., Fleming, M., Algora, A., Angelone, M., Archier, P., Bauge, E., Bersillon, O., Blokhin, A., Cantargi, F., Chebboubi, A., Diez, C., Duarte, H., Dupont, E., Dyrda, J., Erasmus, B., Fiorito, L., Fischer, U., Flammini, D., Foligno, D., Gilbert, M.R., Granada, J.R., Haeck, W., Hamsch, F.-J., Helgesson, P., Hilaire, S., Hill, I., Hursin, M., Ichou, R., Jacqmin, R., Jansky, B., Jouanne, C., Kellett, M.A., Kim, D.H., Kim, H.I., Kodeli, I., Koning, A.J., Konobeyev, A.Yu.,

- Kopecky, Kos, B., Krása, A., Leal, L.C., Leclaire, N., Leconte, P., Lee, Y.O., Leeb, H., Litaize, O., Majerle, M., I Márquez Damián, J., Michel-Sendis, F., Mills, R.W., Morillon, B., Noguère, G., Pecchia, M., Pelloni, S., Pereslavtsev, P., Perry, R.J., Rochman, D., Röhrmoser, A., Romain, P., Romojaro, P., Roubtsov, D., Sauvan, P., Schillebeeckx, P., Schmidt, K.H., Serot, O., Simakov, S., Sirakov, I., Sjöstrand, H., Stankovskiy, A., Sublet, J.C., Tamagno, P., Trkov, A., van der Marck, S., Álvarez-Velarde, F., Villari, R., Ware, T.C., Yokoyama, K., Žerovnik, G., 2006. The joint evaluated fission and fusion nuclear data library, JEFF-3.3. *Eur. Phys. J. A* 56 (181). <https://doi.org/10.1140/epja/s10050-020-00141-9>.
- Reilly, D., Ensslin, N., Smith, H., Jr., 1991. Passive Nondestructive Assay of Nuclear Materials (Tech. Rep. LA-UR-90-732). Los Alamos National Laboratory, Los Alamos, NM, USA.
- Rinard, P.M., Menlove, H.O., 1996. Application of Curium Measurements for Safeguarding at Reprocessing Plants, Tech. Rep. LA-13134-MS. Los Alamos National Laboratory, Los Alamos, NM, USA.
- Rinard, P.M., Bosler, G.E., 1998. Safeguarding LWR Spent Fuel With the Fork Detector, Tech. Rep. LA-11096-MS, Los Alamos National Laboratory, Los Alamos, NM, USA.
- Rochman, D., Sciolla, C.M., 2014. Nuclear Data Uncertainty Propagation for a Typical PWR Fuel Assembly with Burnup. *Nucl. Eng. Technol.* 46 (3), 353–362. <https://doi.org/10.5516/NET.01.2014.712>.
- Rossa, R., Borella, A., 2020. Development of the SCK CEN reference datasets for spent fuel safeguards research and development. *Data Brief* 30, 105462. <https://doi.org/10.1016/j.dib.2020.105462>.
- Rossa, R., Borella, A., van der Meer, K., 2013. Development of a reference spent fuel library of 17x17 PWR fuel assemblies. *ESARDA Bull.* 49, 27–39.
- Sampson, T.E., 1991. Plutonium Isotopic Composition by Gamma-Ray Spectroscopy. In: D. Reilly, N. Ensslin, H. Smith, Jr. (Eds.), *Passive Nondestructive Assay of Nuclear Materials*, Office of Nuclear Regulatory Research, Washington, DC, USA, Ch. 8, p. 228.
- Sasahara, A., Matsumura, T., Nicolaou, G., Kiyonagi, Y., 2008. Isotopic Analysis of Actinides and Fission Products in LWR High-Burnup UO₂ Spent Fuels and its Comparison with Nuclide Composition Calculated Using JENDL, ENDF/B, JEF and JEFF. *J. Nucl. Sci. Technol.* 45 (4), 313–327. <https://doi.org/10.1080/18811248.2008.9711440>.
- Schillebeeckx, P., Verwerft, M., Žerovnik, G., Parthoens, Y., Pedersen, B., Alaerts, G., Cools, G., Govers, K., Paepen, J., Varasano, G., Wynants, R., 2020. A non-destructive method to determine the neutron production rate of a sample of spent nuclear fuel under standard controlled area conditions (Tech. Rep. RC121586). Joint Research Centre, Geel, Belgium.
- Shin, T.H., Bravo, C.A., Marlow, J., Geist, W., Clarke, S.D., Pozzi, S.A., 2019. Neutron-neutron angular and energy-angle correlations of plutonium samples with varying α ratio. *Nucl. Instrum. Meth. A* 946, . <https://doi.org/10.1016/j.nima.2019.06.038> 162297.
- Simakov, S.P., van den Berg, Q.Y., 2017. Update of the – n Yields for Reactor Fuel Materials for the Interest of Nuclear Safeguards. *Nucl. Data Sheets* 139, 190–203. <https://doi.org/10.1016/j.nds.2017.01.005>.
- Simakov, S.P., Verpelli, M., Otsuka, N., 2015. Update of the nuclear data for the neutron emissions for actinides of interest in safeguards (Tech. rep.). Nuclear Data Section, International Atomic Energy Agency.
- Stankus, S.V., Khairulin, R.A., Mozgovoy, A.G., Roshchupkin, V.V., Pokrasin, M.A., 2008. The density and thermal expansion of eutectic alloys of lead with bismuth and lithium in condensed state. *J. Phys.: Conf. Ser.* 98, . <https://doi.org/10.1088/1742-6596/98/6/062017> 062017.
- Tobin, S.J., Menlove, H.O., Swinhoe, M.T., Blanc, P., Burr, T., Evans, L.G., Favalli, A., Fensin, M.L., Freeman, C.R., Galloway, J., Gerhart, J., Rajasingam, A., Rauch, E., Sandoval, N.P., Trellue, H., Ulrich, T.J., Conlin, J.L., Croft, S., Hendricks, J., Henzl, V., Henzlova, D., Eigenbrodt, J.M., Koehler, W.E., Schear, M.A., Lee, D.W., Lee, T. H., Schear, M.A., Humphrey, M.A., Smith, L.E., Anderson, K.K., Campbell, L.W., Casella, A., Gesh, C., Shaver, M.W., Misner, A., Amber, S.D., Ludewigt, B.A., Quiter, B., Solodov, A., Charlton, W., Eigenbrodt, J.M., Stafford, A., LaFleur, A.M., Romano, C., Cheatham, J., Ehinger, M., Thompson, S.J., Chichester, D.L., Sterbent, J.L., Hu, J., Hunt, A., Koehler, W.E., Lee, T.H., Mozin, V., Richard, J.G., Smith, L.E., 2012. Technical cross-cutting issues for the next generation safeguards initiative's spent fuel nondestructive assay project. *J. Nucl. Mater. Manag.* 40 (3), 18–24.
- Tsvetkov, P.V., Waltar, A.E., Todd, D.R., 2012. Sustainable Development of Nuclear Energy and the Role of Fast Spectrum Reactors. In: A.E. Waltar, D.R. Todd, P.V. Tsvetkov (Eds.), *Fast Spectrum Reactors*, Springer, Boston, MA, USA, Ch. 1.
- U.S. Energy Information Administration, 2021. Annual commercial spent fuel discharges and burnup, 1968–2017, accessed on July 7, 2021. URL: https://www.eia.gov/nuclear/spent_fuel/ussnftab3.php.
- Vaccaro, S., Tobin, S.J., Favalli, A., Grogan, B., Jansson, P., Liljenfeldt, H., Mozin, V., Hu, J., Schwalbach, P., Sj, A., 2016. PWR and BWR spent fuel assembly gamma spectra measurements. *Nucl. Instrum. Meth. A* 833, 208–225. <https://doi.org/10.1016/j.nima.2016.07.032>.
- Van den Eynde, G., Malambu, E., Stankovskiy, A., Fernandez, R., Baeten, P., 2015. An updated core design for the multi-purpose irradiation facility MYRRHA. *J. Nucl. Sci. Technol.* 52, 1053–1057. <https://doi.org/10.1080/00223131.2015.1026860>.
- Van Tichelen, K., Kennedy, G., Mirelli, F., Marino, A., Toti, A., Rozzia, D., Cascioli, E., Keijers, S., Planquart, P., 2020. Advanced Liquid-Metal Thermal-Hydraulic Research for MYRRHA. *Nucl. Technol.* 206, 150–163. <https://doi.org/10.1080/00295450.2019.1614803>.
- Weisenburger, A., Schroer, C., Jianu, A., Heinzel, A., Konys, J., Steiner, H., Müller, G., Fazio, C., Gessi, A., Babayan, S., Kobzova, A., Martinelli, L., Ginestar, K., Balbaud-Célièrier, F., Martín-Muñoz, F.J., Soler Crespo, L., 2011. Long term corrosion on T91 and AISI1 316L steel in flowing lead alloy and corrosion protection barrier development: experiments and models. *J. Nucl. Mater.* 415(3), 260–269. doi: 10.1016/j.jnucmat.2011.04.028.
- Willman, C., 2006. Applications of Gamma Ray Spectroscopy of Spent Nuclear Fuel for Safeguards and Encapsulation (Ph.D. thesis). Uppsala Universitet, Uppsala, Sweden.